SYNTHESIS OF ZEOLITE FROM COAL FLY ASH WITH ALUMINUM DROSS USING ALKALI FUSION

Miss Napasawan Khawnuan

A Thesis Submitted in Partial Fulfillment of the Requirements

for the Degree of Master of Science Program in Environmental Management

(Interdisciplinary Program)

Graduate School

Chulalongkorn University

Academic Year 2011

Copyright of Chulalongkorn University

การสังเคราะห์ซีโอไลต์จากเถ้าลอยถ่านหินผสมกับตะกรันอลูมิเนียมด้วยวิธีอัลคาไลน์ฟิวชั่น

นางสาวนภัสวัลย์ ขาวนวล

Thesis Title	SYNTHESIS OF ZEOLITE FROM COAL FLY ASH WITH ALUMINUM DROSS USING ALKALI FUSION
By	Miss Napasawan Khawnuan
Field of Study	Environmental Management
Thesis Advisor	Assistant Professor Manaskorn Rachakornkij, Ph.D.
Thesis Co-advisor	Thantip Punmatharith, Ph.D.

Accepted by the Graduate School, Chulalongkorn University in Partial Fulfillment of the Requirements for the Master's Degree

………………………………….... Dean of the Graduate School

(Associate Professor Pornpote Piumsomboon, Ph.D.)

THESIS COMMITTEE

………..……………………….. Chairman
(Assistant Professor Chantra Tongcumpou, Ph.D.)

…………………………………… Thesis Advisor
(Assistant Professor Manaskorn Rachakornkij, Ph.D.)

…………………………………… Thesis Co-advisor
(Thantip Punmatharith, Ph.D.)

…………………………………. Examiner
(Assistant Professor Patiparn Punypalakul, Ph.D.)

…………………………………. External Examiner
(Pattamawan Khunprasert, Ph.D.)

นภัสวัลย์ ขาวนวล : การสังเคราะห์ซีโอไลต์จากเถ้าลอยถ่านหินผสมกับตะกรันอลูมิเนียม ด้วยวิธีอัลคาไลน์ฟิวชั่น (SYNTHESIS OF ZEOLITE FROM COAL FLY ASH WITH ALUMINUM DROSS USING ALKALI FUSION) อ.ที่ปรึกษาวิทยานิพนธ์หลัก: ผศ. ดร. มนัสกร ราชากรกิจ, อ.ที่ปรึกษาวิทยานิพนธ์ร่วม: ดร. ธารทิพย์ พันธ์เมธาฤทธิ์, 77 หน้า.

เถ้าลอยถ่านหินและกากตะกรันอลูมิเนียมจัดเป็นของเสียจากอุตสาหกรรม ซึ่งจำเป็นต้องมี การกำจัดอย่างถูกวิธี งานวิจัยหลายชิ้นมุ่งเน้นไปที่การนำเถ้าลอยถ่านหินไปใช้เป็นสารตั้งต้นในการ ผลิตซีโอไลต์ อย่างไรก็ตามการประยุกต์ใช้กากตะกรันอลูมิเนียมในการสังเคราะห์ซีโอไลต์ยังไม่ได้ มีการศึกษา ในงานวิจัยนี้ได้มีการใช้เถ้าลอยถ่านหินและกากตะกรันอลูมิเนียมในการสังเคราะห์ ซีโอไลต์ด้วยวิธีอัลคาไลน์ฟิวชั่น โดยนำอลูมินัมออกไซด์ซึ่งเป็นวัตถุดิบที่นิยมใช้ในการสังเคราะห์ ซีโอไลต์มาใช้ทดสอบเปรียบเทียบกับกากตะกรันอลูมิเนียม มีการศึกษาหาสภาวะที่เหมาะสมใน การสังเคราะห์ซีโอไลต์โดยเปรียบเทียบจากลักษณะสมบัติของซีโอไลต์ที่สังเคราะห์ได้ เช่น ความ สามารถในการแลกเปลี่ยนไอออนบวก (ซีอีซี) ซึ่งจากการทดลองพบว่า สามารถสังเคราะห์ซีโอไลต์ เอ เมื่อใช้กากตะกรันอลูมิเนียมที่สภาวะเหมาะสมคือ อุณหภูมิฟิวชั่นที่ 600 องศาเซลเซียส ตามด้วย อุณหภูมิในการตกผลึกที่ 80 องศาเซลเซียส พบว่าค่าซีอีซีที่ได้จากตัวอย่างนี้จะมีค่าใกล้เคียงกันกับ ค่าของตัวอย่างซีโอไลต์ที่สังเคราะห์ได้จากอลูมินัมออกไซด์ จากนั้นได้นำซีโอไลต์ที่สังเคราะห์ได้ ที่ซึ่งมีค่าซีอีซีสูง (P680 P780 D680 และ D780) ไปศึกษาการดูดซับของสารละลายแคดเมียมและ เมทิลีนบลู และจากการใช้แบบจำลองทั้งสามแบบ ซึ่งประกอบไปด้วย ความสัมพันธ์แบบเส้นตรง ไอโซเทอมแลงเมียร์ และไอโซเทอมฟรุนดลิค พบว่าพฤติกรรมการดูดซับแคดเมียมด้วยซีโอไลต์ที่ สังเคราะห์ได้นั้น สามารถอธิบายได้ด้วยแบบจำลองฟรุนดลิค ส่วนการดูดซับของเมทิลีนบลูนั้น ไม่ สามารถอธิบายได้ด้วยแบบจำลองที่ใช้ในการทดลองนี้ได้ จากการทดลองพบว่า เถ้าลอยถ่านหิน และกากตะกรันอลูเนียมสามารถนำมาสังเคราะห์ซีโอไลต์เอ ที่มีความสามารถในการดูดซับ แคดเมียมและเมทิลีนบลูได้ใกล้เคียงกับซีโอไลต์ที่สังเคราะห์ได้จากเถ้าลอยถ่านหินและอลูมินัม ออกไซด์

สาขาวิชา การจัดการสิ่งแวดล้อม   ลายมือชื่อนิสิต _____

ปีการศึกษา 2554   ลายมือชื่อ อ.ที่ปรึกษาวิทยานิพนธ์หลัก _____

ลายมือชื่อ อ.ที่ปรึกษาวิทยานิพนธ์ร่วม _____

5287538320 : MAJOR   ENVIRONMENTAL MANAGEMENT
KEYWORDS : ZEOLITE / COAL FLY ASH / ALUMINUM DROSS / CADMIUM / METHYLENE BLUE

NAPASAWAN KHAWNUAN: SYNTHESIS OF ZEOLITE FROM COAL FLY ASH WITH ALUMINUM DROSS USING ALKALI FUSION. ADVISOR: ASST. PROF. MANASKORN RACHAKORNKIJ, Ph.D., CO-ADVISOR: THANTIP PUNMATHARITH, Ph.D., 77 pp.

Coal fly ash (CFA) and aluminum dross are industrial wastes that required proper treatment and disposal. Several studies have been focusing on reusing CFA to produce zeolites; a porous crystalline materials with various applications. Nonetheless, the applicability of aluminum dross in zeolite synthesis has yet to be determined. In this study, CFA and aluminum dross were used for the synthesis of zeolite by akaline fusion. Aluminum oxide, a commonly used aluminum source, was also tested for comparison. Optimal condition of zeolite synthesis was determined based on characteristics of the products such as cation exchange capacity (CEC). Zeolite A was generated in this study. In the case of aluminum dross, optimal synthesis condition was obtained at 600 ˚C fusion temperature followed by crystallization at 80 ˚C. Although the observed CEC was relatively lower than those of the zeolites synthesized from aluminum oxide, their CEC values were still comparable. The cadmium and methylene blue (MB) adsorptions of the synthesized zeolites with high CEC values (P680, P780, D680, and D780) were then investigated. Among the three isotherm models including linear regression, Langmuir isotherm, and Freundlich isotherm, the data from cadmium adsorption by the synthesized zeolites fitted well with the Freundlich isotherm. On the contrary, MB adsorption could not be fitted with any models used in this study. These results suggest that zeolite A can be obtained from CFA and aluminum dross, and its capability in cadmium and MB removal was similar to the zeolite produced from aluminum oxide.

Field of Study: Environmental Management   Student's Signature………………………

Academic Year: 2011   Advisor's Signature………………………

                                                                          Co-advisor's Signature…………………...

ACKNOWLEDGEMENTS

CONTENTS

LIST OF TABLES

LIST OF FIGURES

CHAPTER I

INTRODUCTION

1.1 Rationale

Nowadays, industry is an important part of human societies. Many developed countries and developing countries depend significantly on it. However, most of the industrial activities including manufacturing, mining, dyeing processes produce large amount of wastes. In Taiwan, 18 million metric tons of industrial wastes are produced each year (500 tons/km^2) (Wei and Huang, 2001). Approximately 7.6 billion tons of industrial solid wastes are generated in USA each year (U.S. Environmental Protection Agency, 2012). In 2010, about 2.44 million tons of industrial hazardous wastes were estimated in Thailand (Pollution Control Department, Ministry of Natural Resources and Environment, 2010). Normally, industrial solid wastes and industrial hazardous wastes are dumped into landfills and secure landfills, respectively.

Allocating appropriate areas for landfill site is challenging in many countries due to high population density and limited space. Although incineration is a new alternative for eliminating industrial solid wastes that required less space, there are still some remaining residues that need to be disposed into landfills. Due to the limitation of landfill and incineration, improvement in waste management strategies including the implementation of three Rs is crucial.

The three Rs consists of reduce, reuse and recycle (Wimmer et al., 2009). Reuse and recycle are often applied in removing general industrial wastes. The examples of these wastes are waste paper, waste iron, coal ash, tempered high furnace bricks (cinder), sweetening dregs, wood (whole/part), glass (whole/part), bleaching earth ceramics (pottery, brick, tile and cast sand), metal scraps (copper, zinc, aluminum and tin) and plastics (Wei and Huang, 2001). Many industrial products are produced through recycling of industrial wastes. For instance, plastic waste can be recycled into raw materials for petrochemical processes, new plastic production, and alternative fuel production (Kang and Schoenung, 2005). These newly generated products from industrial wastes also include zeolite; a well known environmental remediation tool capable of removing various toxic contamination.

Zeolites are crystalline aluminosilicates of group I or group II elements. These zeolites are used widely in various industrial applications due to their variety of pore sizes, structures and surface areas. These applications include using zeolites in ion exchange, gas adsorption, water adsorption and catalysts (Breck, 1974; Querol et al., 2002). In order to reduce the cost of zeolites and make the zeolite-involved processes more cost effective, many studies focused their efforts in synthesizing zeolites from various industrial wastes such as oil shale ash, waste porcelain, waste metals and coal

fly ash (CFA) (Fernandes et al., 2005; Wajima and Ikegami, 2009; Hiraki et al., 2009; Belviso et al., 2010). These wastes contain silicon and aluminum that are necessary for the synthesis of zeolite. Therefore, several studies used CFA in the production of zeolite due to its high silicon composition (Shigemoto et al., 1993; Querol et al., 2002; Tanaka et al., 2004; Yaping et al., 2008; Tanaka and Fujii, 2009; Belviso et al., 2010).

CFA is one of the solid wastes generated from the electrical power plant, and approximately 500 million tons of CFA are discharged worldwide each year (Wang et al., 2008). About 3 million tons of CFA were produced in Mae Moh, Thailand (Wimolmala et al., 2004). Generally, CFA is dumped into landfills, which leads to serious environmental problems due to its alkalinity and fine particle size. Since CFA composes mainly of amorphous aluminosilicate and some crystals such as quartz, mullite, hematite and magnetite, it can be employed as raw materials for zeolite production by serving as silicon source. The synthesis of zeolites using CFA has been widely studied, explored and developed in the last few decades (Shigemoto et al., 1993; Querol et al., 2002; Tanaka et al., 2004; Yaping et al., 2008; Tanaka and Fujii, 2009; Belviso et al., 2010).

Chemical grade aluminum (aluminum oxide, Al_2O_3 and sodium aluminate, $NaAlO_2$) are commonly used for the synthesis of zeolite. Nonetheless, in this study, potential use of aluminum dross as a substitution of chemical grade aluminum in zeolite synthesis was investigated. Aluminum dross is a waste from the aluminum recycling industry, and about five million tons of aluminum dross is discharged globally (Chandrasekar et al., 2009). The disposal of aluminum dross has become a serious concern. Conventionally, these wastes are disposed in landfill sites, which may lead to ground water contamination if leaching occurs (Murayama et al., 2009). Moreover, aluminum dross can react with water producing harmful gases such as ammonia, methane, hydrogen and hydrogen sulfide into the atmosphere (Shinzato and Hypolito, 2005). Therefore, many efforts have been focused on new techniques to utilize this waste. One of these efforts was to use aluminum dross as raw material for producing adsorbents and catalysts such as zeolites and zeotype materials (Murayama et al., 2006; Dash et al., 2008; Chandrasekar et al., 2009; Hiraki et al., 2009; Murayama et al., 2009).

The aim of this study is to utilize two industrial wastes, CFA and aluminum dross, to produce synthetic zeolites. Previous studies found that CFA can be used as silicon source for zeolite synthesis (Berkgaut and Singer, 1996; Hui and Chao, 2006; Gross-Lorgouilloux et al., 2010). Usually, chemical grade aluminum is used as source of aluminum (Shih and Chang, 1996; Wang, Li, Sun et al., 2009; Fotovat et al., 2009; Kazemian et al., 2010); however, in this study, aluminum dross was used instead. Normally, zeolites are synthesized from two major methods: hydrothermal and fusion methods. For the products from fusion method exhibit higher cation exchange

capacity (CEC) (Molina and Poole, 2004), fusion method was chosen for this study. The ability of the synthesized zeolites in cadmium and methylene blue (MB) removal was then experimented.

1.2 Objectives

The main objective of this study is to synthesize zeolite from CFA with aluminum dross using alkali fusion. Two sub-objectives of this study are as the followings:

- To investigate physical and chemical properties of the synthesized zeolite.
- To apply the synthesized zeolite for removal of cadmium and MB solution.

1.3 Hypotheses

1. CFA and aluminum dross can be used as raw materials to produce zeolite by alkali fusion method.
2. Chemical and physical properties of the zeolites synthesized from aluminum dross are comparable to those from chemical grade aluminum (Al_2O_3).
3. Obtained zeolite can remove cadmium and MB solution.

1.4 Scope of the study

This study consists of four parts: Raw material analysis, Zeolite synthesis, Characterization of synthesized zeolite and Application of synthesized zeolite.

1. Raw material analysis

CFA and aluminum dross were randomly collected from Siam City Cement Public Company Limited and local aluminum recycling company in Ayutthaya province, respectively. The chemical and physical properties of CFA were investigated for:

- Chemical composition: by X-Ray Fluorescence Spectrometer (XRF).
- Crystalline structure: by X-Ray Diffractometer (XRD).
- Total metal composition: by microwave and Inductively Coupled Plasma (ICP).
- pH (1:10 CFA/water suspensions): by pH meter.
- Moisture content: by ASTM D 2216-98.
- Loss on ignition (LOI): by ASTM D 7348-07.
- CEC: by ammonium acetate method.

Aluminum dross was analyzed for:

- Chemical composition: by XRF.

- Crystalline structure: by XRD.
- Total metal composition: by microwave and ICP.
- pH (1:10 aluminum dross /water suspensions): by pH meter.

2. Zeolite synthesis

2.1 In order to synthesize zeolite from CFA with aluminum dross, alkali fusion method was employed in this study. The condition for zeolite synthesis is as follows:
- The fusion temperature was varied at 550 °C, 600 °C, 700 °C, or 800 °C
- The crystallization temperature was varied at 80 °C and 100 °C.
- The reaction time for fusion, aging and crystallization process was set at 60 minutes, 24 hours and 12 hours, respectively.

2.2 The ratio of silica to aluminum to NaOH for synthesizing zeolite was 1:1:1.2. CFA was used as source of silica, whereas aluminum content was obtained from both CFA and aluminum oxide/aluminum dross.

3. Characterization of synthesized zeolite

3.1 Optimal condition for synthesizing zeolite using alkali fusion method was determined based on CEC of the synthesized zeolite by ammonium acetate method.
3.2 Chemical and physical properties of the synthesized zeolite were investigated:
- Chemical composition: by XRF
- Crystalline structure: by XRD
- Morphology: by Scanning Electron Microscope (SEM)
- Specific surface area (SSA): by BET

4. Application of synthesized zeolite

4.1 Removal of cadmium solution
4.2 Removal of MB solution

1.5 Expected outcomes

Both aluminum dross and CFA can be used for the synthesis of zeolites to obtain the desired type of zeolite, and the synthesized zeolites can be applied for the removal of cadmium and MB.

CHAPTER II

THEORETICAL BACKGROUND AND LITERATURE REVIEW

2.1 Zeolite

2.1.1 Structure of zeolite

Zeolites are crystalline aluminosilicates of group I or ground II elements. The atomic unit of zeolites composed of one silicon or one aluminum atom and four oxygen atom (SiO_4 or AlO_4). These atom of zeolites are linked together forming a tetrahedral structure of $[AlO_4]^{-5}$ or $[SiO_4]^{-4}$ (Figure 2.1). This structure is generally referred as Primary Building Unit (PBU). Inside the PBU, there are voids and opened spaces, which are occupied by cation and water molecules. The cation contained in PBU can be replaced by other cation during an ion exchange process (Breck, 1974; Querol et al., 2002). A tetrahedral stucture of Al^{3+} or Si^{4+} central atom surrounded by four oxygen atoms results in a negative charge of the molecule. This negative charge is balanced by a cation such as sodium. The cationic ions are exchangable with other cations including heavy metals (Jamil et al., 2011).
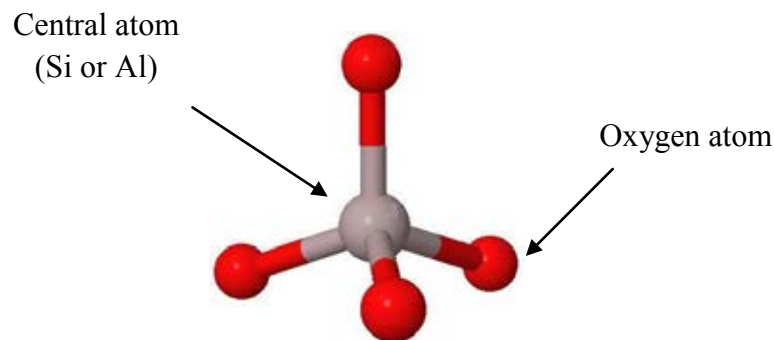
Figure 2.1 Primary Building Unit (PBU) of zeolite

The unit cell formula of zeolite is presented as follows:

$$M_{x/n} [(Al_2O_3)_x (SiO_2)_y].w \ H_2O$$
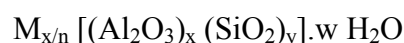
Where M represents the cation with n valency, whereas x and y are numbers of primary building unit with aluminum and silicon as a center atom, respectively. Moreover, w is a number of water molecule in the unit cell (Apiratikul, 2006).

The larger and more complex structure of zeolite is considered as secondary building unit (SBU), which comprises of several PBUs (Figure 2.2). Furthermore, zeolites with even more complex structure are classified as structural subunit (SSU) (Figure 2.3).
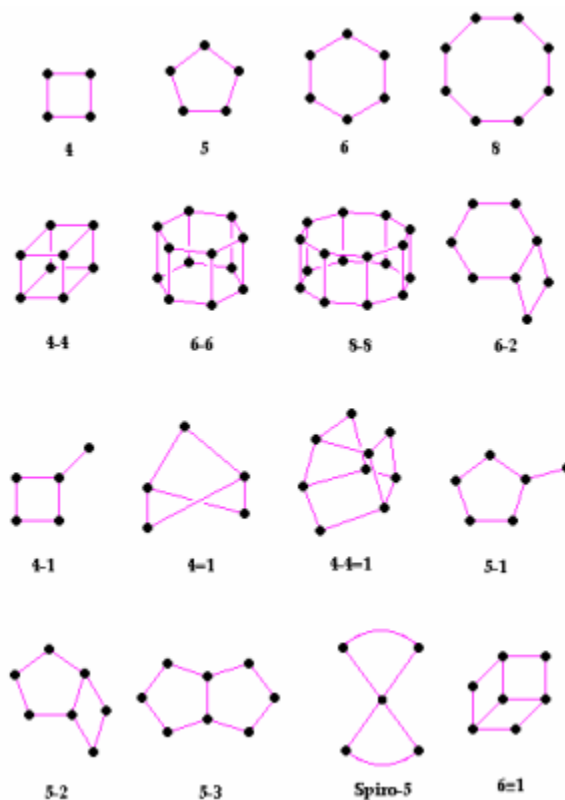
Figure 2.2 Secondary Building Unit (SBU) of zeolite
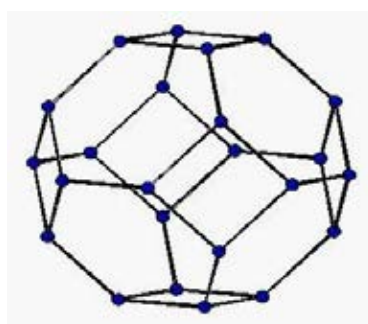
β - cages

Figure 2.3 Structural Sub Unit (SSU) of zeolite

2.1.2 Type of zeolite

2.1.2.1 Natural zeolite

Zeolites were first discovered in 1756 by a Swedish mineralogist, Cronstedt. In nature, zeolites are formed from the reaction of volcanic rocks, ashes, and alkaline groundwater. Over thousands to millions years of crystallization process are required to generate natural zeolites. There are currently more than 40 natural zeolites identified according to their chemical compositions, structures, and related physical properties. Some examples these zeolites are analcime, chabazite, clinoptilolite, phillipsite, stilbnite, mordenite, heulandite and natrolite. Natural zeolites can be used as an adsorbent and ion-exchanger, which are also safe and environmentally friendly. However, natural zeolites are rarely pure, varying in chemical composition and less uniformity. They are generally contaminated by other metals, minerals, amorphous glasses, quartzes or other zeolites (Breck, 1974). As a result, the synthetic zeolites are commonly used instead.

2.1.2.2 Synthetic zeolite

Synthetic zeolites with high purity were first produced in the 1950sMore than 150 different zeolites including zeolite A, X, Y and P have been identified so far. Characteristics of the synthetic zeolites such as their composition, structure and pore size can be varied by different production conditions. Hence, wide variety of zeolites was used in many industrial applications.

The least complex structure of synthetic zeolite is found in zeolite A. The molecular ratio of zeolite A is the one silicon to the one aluminum (Si/Al), and there are three forms of such zeolites including 3A, 4A and 5A. These forms of zeolite A were classified based on their pore sizes. Zeolite 3A has a pore size of approximately 3 angstrom, and its unit cell is $0.4K_2O^.0.6Na_2O^.Al_2O_3^.2.0SiO_2^.4.5H_2O$. Zeolite 4A is the form of Na with approximately 4 angstrom pore opening. The unit cell of this zeolite is $Na_{12}[(AlO_2)_{12}(SiO_2)_{12}]\cdot27H_2O$. Zeolite 4A is the most commonly used because of its various applications. When one calcium ion exchanges with two sodium ions, the pore size increases to approximately 5 angstrom. This type of zeolite is zeolite 5A, which consists of $0.7CaO\cdot0.3Na_2O\cdot Al_2O_3\cdot2.0SiO_2\cdot4.5H_2O$. Zeolite A has a cubic symmetry and a density of 1.99 g/ml.

2.2 Coal fly ash (CFA)

CFA is a waste material generated during the combustion process of coal. It is usually collected from electrostatic precipitators, baghouses, or mechanical devices such as cyclone (Tanaka and Fujii, 2009). CFA is generally categorized based on its chemical composition into two different classes; class F and class C by ASTM C618 method. Class F fly ash is normally produced by burning anthracite and bituminous

coals that contains less than 10% lime (CaO). Class C fly ash is normally generated by incineration of lignite and sub-bituminous coals that contains more than 20% lime CaO (Tu et al., 2009).

Most of the CFA particles are round and spherical with the size ranging from 1 to 100 μm (Yaping et al., 2008). The color is vaired from light brown to gray color depending on the amount of carbon in the coal. More than 20% of CFA is a cenosphere (hollow spheres), and the chemical compositions are dependent on the combustion conditions and the type of coal used (Apiratikul, 2006). The major elemental components are silicon, aluminum, ferrous and calcium (95-99% by weight). Beside these major components, CFA consists of several other elements including magnesium, titanium, sodium, potassium, sulfur and phosphorus (0.5-3.5% by weight) (Phanphaisan, 2006). In addition, CFA is also composes of various heavy metals such as arsenic, lead, tin and cadmium (Tanaka and Fujii, 2009).

The crystallography of CFA contains mainly amorphous aluminosilicate (glass phase) with some crystals such as α-quartz (SiO_2), mullite ($2SiO_2 \cdot 3Al_2O_3$), hematite (α-Fe_2O_3) and magnetite (Fe_3O_4) (Tanaka and Fujii, 2009). The glass phase contributes to approximately 60-80% of fly ash, and serves as silicon and aluminum sources (Berkgaut and Singer, 1996).

Although CFA has a pozzolanic property and can be applied as raw material for cement manufacturing, only 20% of fly ash is used and the remaining is normally disposed into landfills (Wang, Li, Sun et al., 2009). This leads to many environmental concerns since CFA in landfills can pollute soil and groundwater due to its toxicity. Thus, many studies have been focusing on developing new alternative application of CFA (Yaping et al., 2008). Due to the high content of silicon and aluminum, CFA is potentially suitable for zeolite synthesis.

2.3 Aluminum dross

According to the prominent properties of aluminum, it has been widely used in many industries such as transportation, packaging, medicine, electronic and construction. The growth in aluminum usages causes significant increase in aluminum wastes from the aluminum production and recycling (Murayama et al., 2009). The recycling process generates aluminum dross (white dross and black dross) and salt cake as shown in Figure 2.4 and 2.5. White dross and black dross are classified by their metal content (Manfredi et al., 1997). White dross (or wet dross) has a high aluminum content and low oxides and salts, which tends to be recycled for aluminum. Black dross (or dry dross) has a low aluminum content and high oxides and salts, and tends to be refined for lower quality white dross. The color and shape of aluminum dross are gray to black and granules (Figure 2.6), respectively. It also emits an odor of ammonia and has specific gravity of 2.5 to 2.9 (CAMEO chemicals, 2010).
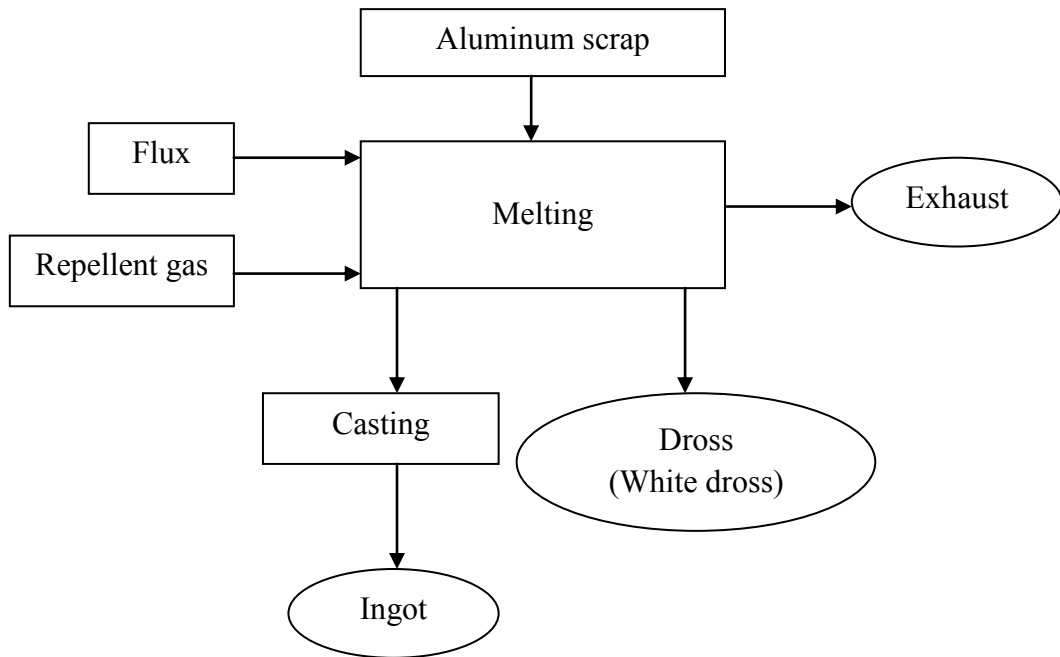
Figure 2.4 Melting and Casting aluminum process
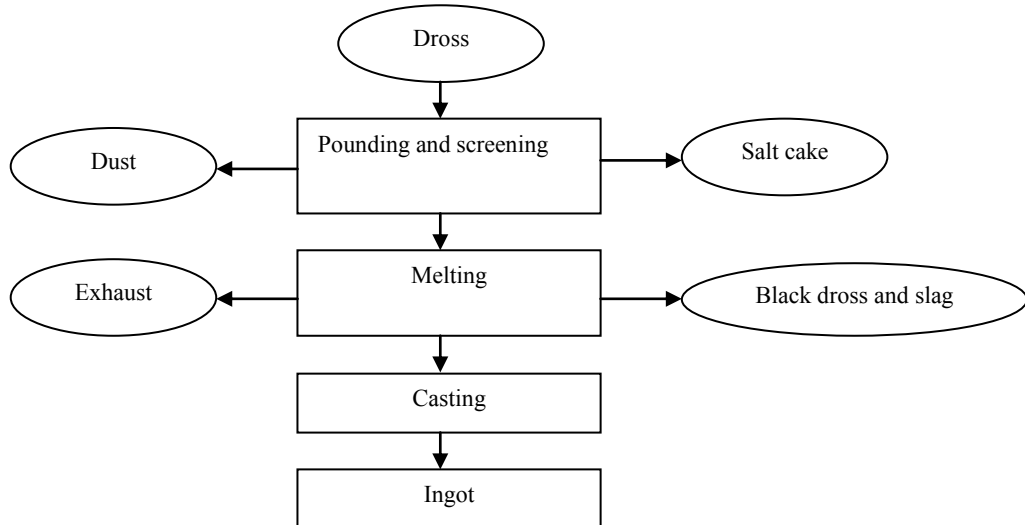
Figure 2.5 Melting and Casting aluminum dross process

Figure 2.6 Aluminum dross (black dross and white dross) (JBMI Group Ltd, 2010: online)

When aluminum dross contacts with water, toxic and flammable gases are generated. Therefore, normally in the disposal of aluminum dross in landfill is managed in order to prevent the contact between dross and water. Aluminum dross consists of free metal, salts oxides, and other nonmetallic substances such as Al_2O_3, aluminum nitride (AlN), aluminum carbide (Al_4C_3) and aluminum sulfide (Al_2S_3) (Manfredi et al., 1997; Dash et al., 2008; Chandrasekar et al., 2009). The hydrolysis of aluminum metal, nitrides, carbides, and sulfides generates toxic and inflammable gases including hydrogen (H_2), ammonia (NH_3), methane (CH_4), and hydrogen sulfide (H_2S) (equation 2.1-2.4) (Shinzato and Hypolito, 2005; David and Kopac, 2012).

$$2Al+2H_2O+4OH^- \rightarrow 2Al(OH)_3+H_2 \qquad (2.1)$$

$$2AlN+6H_2O \rightarrow 2Al(OH)_3+2NH_3 \qquad (2.2)$$

$$Al_4C_3+12H_2O \rightarrow 4Al(OH)_3+3CH_4 \qquad (2.3)$$

$$Al_2S_3+6H_2O \rightarrow 2Al(OH)_3+3H_2S \qquad (2.4)$$
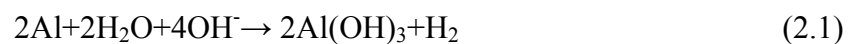
Inhalation or contact with high concentration of ammonia gas may cause harmful effects to human such as severe eye irritation. Methane is believed to be a significant contributor to global warming (Ewais et al., 2009).

2.4 Cadmium

Cadmium (Cd) has long been known as one of the most toxic elements to the environment and human health. Several studies suggested that cadmium may increase the risk of cancer, kidney dysfunction, bone fraction, and other pulmonary, gastrointestinal, and liver diseases (Waalkes, 2003; Engström et al., 2012; Järup and Åkesson, 2009). Although cadmium may not directly damage DNA inside living organisms, studies suggested that it may interfere with cellular functions and generate reactive oxygen species (ROS), which in turn cause damage to DNA (Bertin and Averbeck, 2006; Filipič, 2011). Certain levels of cadmium may be naturally found in the environment. However, significant contamination in the environment is resulted from many human related activities including mining operation, use of phosphate fertilizers, and battery production. Normally, cadmium is non-soluble in water, but soluble in acids including nitric acid, sulfuric acid, and hydrochloric acid. Study also reported that cadmium can be accumulated in several edible plants and grains, which may lead to human and animal ingestion of cadmium (Järup and Åkesson, 2009). With long half-life, cadmium is persistent in the environment, and required the uses of remediation approaches to remove them. Many methods were applied and tested for the removal of cadmium (Mulligan et al., 2001; Hashim et al., 2011). Nonetheless, adsorption using zeolite is one of the most suitable approaches due to its cost-effectiveness, high removal efficiency, and environmentally friendly property (Misaelides, 2011).

2.5 Methylene blue (MB)

Methylene blue (MB) is a cationic dye that was first discovered by Caro in 1878 (El Qada et al., 2006). The molecular formula is $C_{16}H_{18}N_3SCl$ as shown in Figure 2.7. MB is a dark green powder and odorless at room temperature. The color becomes blue when dissolved in water. This dye is widely used in coloring processes such as staining procedures and dyeing cottons. However, MB can be harmful on humans and animals. When directly exposed, it may cause dizziness, anemia, mental confusion, hypertension, tachycardia, dyspnea, convulsions, irritation to the skin, and diarrhea (Harvey and Keitt, 1983; Mokhlesi et al., 2003; Senthilkumaar et al., 2005). Therefore, it is important to remove MB from industrial wastewater effluent.
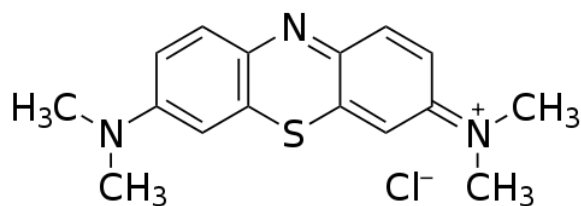
Figure 2.7 Chemical structure of methylene blue

2.6 Adsorption isotherm

2.6.1 Langmuir model

Langmuir equation is a model that is appropriate to homogeneous adsorption. The activation energy of sorption equal in each adsorbed molecule, and there is no reaction between absorbed molecules (Wang and Zhu, 2006). The well-known Langmuir equation is given as: (Wang and Zhu, 2006)

$$q_e = \frac{q_m K_L C_e}{1 + K_L C_e} \qquad (2.5)$$

where:

q_e = sorption capacity (mg/g)

q_m = maximum sorption capacity (mg/g)

K_L = Langmuir adsorption constant representing a relation of adsorbent to adsorbate (L/mg)

C_e = equilibrium concentration of adsorbate in the solution (mg/L)

The linear form of Langmuir equation is presented below:

$$\frac{1}{q_e} = \frac{1}{q_m} + (\frac{1}{q_m K_L})\frac{1}{C_e} \qquad (2.6)$$

2.6.2 Freundlich model

Freundlich equation is usually employed to describe heterogeneous and reversible adsorption. The Frenudlich adsorption equation is shown as follows: (El Qada et al., 2006; Wang and Zhu, 2006)

$$q_e = K_F C_e^{1/n} \qquad (2.7)$$

where:

q_e = amount adsorbed per unit weight of adsorbent (mg/g)

C_e = equilibrium concentration of adsorbate in the solution (mg/L)

K_F (L/g) and n = Freundlich constants that are the indicators of adsorption capacity and adsorption intensity, respectively.

Freundlich equation can be presented by the linear form as shown below:

$$\log q_e = \log K_F + \frac{1}{n} \log C_e \qquad (2.8)$$

"K_F" and "n" values can be calculated from the intercept and the slope of the plot between log q_e and log C_e, respectively.

2.7 Literature reviews

2.7.1 Synthesis of zeolite

Zeolite can be synthesized from the starting materials containing silica (SiO_2) and alumina (Al_2O_3) in alkaline solution. Many synthesis methods different types of zeolites were developed (Shih and Chang, 1996; Steenbruggen and Hollman, 1998; Hollman et al., 1999; Querol et al., 2002; Molina and Poole, 2004; Wang, Li, Sun et al., 2009), and various raw materials including fly ash, CFA, waste porcelain, oil shale ash, and lagoon ash were used (Kolay et al., 2001; Fernandes Machado and Malachini Miotto, 2005; Wajima and Ikegami, 2009). These substituted materials were chosen due to their similar compositions to the precursor of natural zeolites. Most of the developed synthesis methods are based on the hydrothermal alkaline method, which can be classified as:

2.7.1.1 Hydrothermal alkaline

The hydrothermal alkaline method, which is normally referred as conventional method, involves dissolution of silicon (Si) and aluminum (Al) from fly ash in alkaline solution at high temperature (Querol et al., 2002). Although the hydrothermal treatment is the most common method used for the synthesizing zeolites, there are many disadvantages of it. The resulting materials was usually hydroxy-sodalite or zeolite P together with the less amount of zeolite X and A (Molina and Poole, 2004).

2.7.1.2 Two-step process method

This method consists of two steps. In the beginning, the mixture of fly ash and NaOH is incubated and filtered to dissolve Si source. The filtrate is then mixed with aluminate solution to adjust Si/Al molar ratio. Then, this mixture is crystallized under static condition using hydrothermal method. The obtained zeolites from two-step process were zeolite A (Wang et al., 2008), Na-P1(Hollman et al., 1999), Na-X (Hollman et al., 1999; Tanaka and Fujii, 2009) and Na-A (Hollman et al., 1999; Tanaka and Fujii, 2009). Moreover, zeolite Na-P1 can be obtained from the residual fly ash from first step by the conventional method (Hollman et al., 1999). Wang et al (2008) found that NaOH concentrations related to crystallization time and particle size distribution of zeolite A.

2.7.1.3 Dry or molten-salt method

Molten-salt method is developed based on the use of salt mixture without any addition of water. However, this method has limitations since it obtained low CEC zeolites and required high temperature in the activation process (Park et al., 2000).

2.7.1.4. Alkali fusion

In contrast to the conventional synthesis process in which the quartz (silica source) and mullite (aluminum source) are transformed to zeolite in one step, the silica and aluminum sources in the raw materials are firstly converted to the more soluble forms (sodium silicate and aluminate) during the fusion process. Then the converted product is subjected into hydrothermal process (Shigemoto et al., 1993; Chang and Shih, 2000). This way, the amount of dissolved Si and Al species in the solution can be increased, and the yield of zeolites is increased as well (Chang and Shih, 2000). Furthermore, the fusion method was found to provide higher CEC than the conventional hydrothermal method in the same condition (Molina and Poole, 2004). Chang and Shih (2000) indicated that the structure of zeolite is dependent on the fusion conditions and ratio of Si/Al molar. Some of the examples of zeolite products are faujasite and zeolite A (Shigemoto et al., 1993; Querol et al., 2002). The

previous studies related to the synthesis of zeolite using fusion method are shown in Table 2.1.

2.7.2 Application of zeolites

Due to variety of pore sizes, structures and surface areas of zeolites, they have been used widely in various industries as adsorbents, molecular sieves and catalysts (Breck, 1974). Many researchers have studied the removal of heavy metals from wastewater, and obtained promising results (Kang et al., 1998; Steenbruggen and Hollman, 1998; Hollman et al., 1999; Álvarez-Ayuso et al., 2003; Hui et al., 2005; Penilla et al., 2006; Sui et al., 2008; Apiratikul and Pavasant, 2008; Wang, Li, Sun et al., 2009; Nascimento et al., 2009). In addition, a study found that synthetic zeolites have potential to immobilize radioactive ions in nuclear wastes (Cs^+) (Shih and Chang, 1996).

When compared to commercial grade zeolite 4A, synthesized zeolite 4A from CFA were effective in removing mixed heavy metal ions (Co^{2+}, Cr^{3+}, Cu^{2+}, Zn^{2+} and Ni^{2+}) (Hui et al., 2005). A study conducted by Wang et al. (2009) revealed that zeolite A synthesized from fly ash was more effective in the removal of Cu^{2+} and Zn^{2+} comparing to zeolite X synthesized from the same fly ash. Therefore, the removal of heavy metal is zeolite-type dependent. Moreover, similar level of removal efficiency to commercial zeolite was observed in the synthesized zeolite A. Sui et al. (2008) found that synthesized zeolite consists of zeolite and nonzeolite components, and both components exhibited important contribution to the sorption of Cr^{3+}.

2.7.2.1 Removal of cadmium by synthetic zeolite

Steenbruggen and Hollman (1998) examined the removal of six heavy metals (Ba^{2+}, Cd^{2+}, Co^{2+}, Cu^{2+}, Ni^{2+}, Pb^{2+} and Zn^{2+}) and NH_4^+ using synthesized zeolite (Na-P1). The result revealed that zeolite products can be applied in the environment as an ion exchange agent. The pilot scale removal of Cu^{2+}, Zn^{2+}, Cd^{2+}, Co^{2+}, Ni^{2+} and Pb^{2+} by synthetic zeolite Na-P1, which was prepared from two CFAs, was investigated, and high removal efficiency was observed (Moreno et al., 2001). A study conducted by Álvarez-Ayuso et al. (2003), suggests that five type s of heavy metals including Cr^{2+}, Ni^{2+}, Zn^{2+}, Cu^{2+} and Cd^{2+} could be treated by natural (clinoptilolite) and synthetic (Na-P1) zeolites (prepared from fly ash). The sorption capacity of synthetic the zeolite is ten times higher than those of natural zeolite. Shawabkeh et al. (2004) suggested that zeolite Na-P1 from oil shale ash can reduce cadmium from 100 mg/L to 4.4 mg/L, whereas lead is reduced to 29.42 mg/L from the same initial concentration. The behavior of sorption of cadmium can be adequately explained by Sips model (Shawabkeh et al., 2004). Apiratikul and Pavasant (2008) studied the sorption of Cu^{2+}, Cd^{2+} and Pb^{2+} by using zeolite X

synthesized from CFA. The result showed that the sorption capacity and removal of three heavy metal ions were affected by both initial concentration and sorbent dose.

2.7.2.2 Removal of MB by synthetic zeolite

The adsorption of MB and alizarin sulfonate (AS) by zeolite (hydroxysodalite) synthesized from fly ash was investigated by Woolare et al. (2002). The sorption of cationic dye (MB) was greater than that observed in anionic dye (AS). It was also found that the the sorption of both dyes are surface area dependent since their molecular sizes were too large to enter the channels inside the zeolites. Furthermre, zeolite P resulted from hydrothermal process using fly ash as starting material was used for treating two cationic dyes, MB and rhodamine B (Wang et al., 2006). The sorption rate and efficiency of both dyes were different due to their structures and properties. This suggested that the sorption using zeolites was dependent on the chemical properties of the targeted waste.

Table 2.1 Synthesis of zeolite by alkali fusion

Raw material	FA:NaOH ratio	Fusion temp/time	DI volume (or fused product/DI)	Operating condition				Type of synthesized zeolite	Reference
				Aging temp/time	Crystallization temp/time	pH of washed solution	Drying temp/time		
CFA	1:1.2	550 °C/1h	100 ml	Not defined /12 h	100 °C/ 6 h	-	100 °C overnight	Na-A Na-X	(Shigemoto et al., 1993)
FA, $Al(OH)_3 \cdot xH_2O$	1:1.2	550 °C/1h	0.2:1	Stirred at room temp/ 24 h	60 °C/ -	-	80 °C/12 h	A and X	(Chang and Shih, 2000)
FA	1:1.2	550 °C/1h	85 ml	Vigorous shaking at room temp/ 24 h	90 °C/ 6 h	10	105 °C/ overnight	X	(Molina and Poole, 2004)
CFA	1:1.2 (10 g/12 g)	550 °C/1h	100 ml	Shaking at room temp/ 12 h	100 °C/ 12 h	-	-	Na-A	(Majchrzak-Kuceba and Nowak, 2005)
Oil shale ash (OSA)	2 g OSA/ 4 g NaOH/ 0.95 g Al_2O_3	350 °C/ 2h	36 ml	at room temp/ 24 h (Stirring 3 h by magnetic before)	100 °C/ 6 & 72 h 100 °C/ 12 h	-	100 °C/24 h	Na-A Na-X	(Fernandes Machado and Malachini Miotto, 2005)
FA, Na_2CO_3	1:1.5	830 °C/1 h	5-50 ml	Not defined/ stirred 30 min	100 °C/ -	10	110 °C/10 h	Na-A Na-P1 Na-X	(Yaping et al., 2008)
MSWCA	1:1.2	550 °C/1h	45 ml	Vigorous shaking at room temp/ 24 h	90 °C/ 6 h	10	105 °C/ overnight	X	(Fan et al., 2008)
HSFA, $NaAlO_2$ (Al source)	1:1.2 & 1:2	600 °C/ 1.5 h	1:5 (20 g fused product/ 100 ml DI)	Stirring at room temp/ 8 h	100 °C/ 12 h	< 10	65 °C/ -	Na-A Na-X Na-Y	(Fotovat et al., 2009)
Porcelain	1:1.2	600 °C/6h	1:4	Shaking at room temp/ 24 h	80 °C/ 12 h	-	60 °C overnight	13X	(Wajima and Ikegami, 2009)

Table 2.1 Synthesis of zeolite by alkali fusion

Raw material	FA::NaOH ratio	Fusion temp/time	DI volume (or fused product/DI)	Operating condition				Type of synthesized zeolite	Reference
				Aging temp/time	Crystallization temp/time	pH of washed solution	Drying temp/time		
CFA	1:1.2	550 °C/1h	- (using seawater and DI)	Not defined/ Stirred for a night	35-90 °C/ 4 days	-	80 °C/12 h	-Faujasite, ZK-5, sodalite (using DI&SW) -A(DI) -X, ZK-5 (SW)	(Belviso et al., 2010)
FA	1:1.2	550 °C/1h	50 ml of 0.2M NaOH	Vigorous shaking at 70 °C / several hours	100 °C/ 4 h (with or without shaking) 120 °C/ 4 h (with or without shaking)	-	60 °C overnight	Na-P1	(Kazemian et al, 2010)
FA (adding 2.823 g NaAlO$_2$ for synthesized zeolite A)	1:1.3 (9 g fly ash)	600 °C/ 1.5 h	0.1725:1	Stirring at 25 °C/ 24 h	100 °C/ 5 h 100 °C/ 24 h	7	100 °C/12 h	A X	(Wang, Li, Wang et al., 2009)

CHAPTER III

METHODOLOGY

3.1 Raw material analysis

CFA was collected from Siam City Cement Public Company Limited, and dried in oven (WTB Binder, FD115 (E2)) at 105 °C for 24 hours until reaching a constant weight. The dried CFA was stored in desiccators until use for material analyses and synthesis of zeolite. Aluminum dross was obtained from a local aluminum recycling company in Ayutthaya province. All aluminum dross was grinded and kept in polypropylene containers prior to analyses and synthesis of zeolite. The raw material material analyses conducted on CFA and/or aluminum dross are presented in Table 3.1.

Table 3.1 Summary of raw material analysis

Parameters	Method and instrument	CFA	Aluminum dross
Chemical composition	X-Ray Fluorescence Spectrometer (XRF) (PANalytical, Axios system)	∫	∫
Crystalline structure	X-Ray Diffractometer (XRD) (Bruker AXS, D8 Advance)	∫	∫
Total metals composition	Microwave (Milestone, ETHOS PRO) and ICP(Varian, Vista MPX Axial)	∫	∫
pH	pH meter (HACH sension1pH meter)	∫	∫
Moisture content	ASTM D 2216-98	∫	-
Loss on ignition (LOI)	ASTM D 7348-07	∫	-
CEC	Ammonium acetate method	∫	-

3.1.1 Chemical composition (X-Ray Fluorescence spectrometer)

The chemical composition of CFA and aluminum dross was investigated by X-Ray Fluorescence spectrometer (XRF). The XRF method is a fast and non-destructive to the sample.

3.1.2 Crystalline structure (X-Ray Diffractometer)

The X-Ray Diffractometer (XRD) was used to determine crystalline phase and structure of CFA and aluminum dross using Cu Kα radiation (λ=0.15406 nm).

3.1.3 Total metal compositions

The total metal compositions of CFA was investigated. The CFA was firstly digested by microwave-assisted acid digestion. Tripicate of 0.25 g samples was prepared and subjected to an acid mixture (1.5 mL of HF 40%, 7 ml of HNO_3 65%, and 1 ml of HCL 37%) in closed Teflon vessels. The temperature was elevated to 240 °C and for 45 minutes. The obtained solution was then filtered through Whatman No. 41 filter paper. The filtrate was kept in polyethylene bottles at 4°C until total metal analysis. The analysis was conducted by inductively coupled plasma spectrometry (ICP).

In order to estimate the total metals composition of aluminum dross, Microwave-assisted acid digestion was applied to digest the samples. Three replicates of 0.5 g samples were weighted and digested with an acid mixture (1 mL of HF 40% and 5 ml of H_3BO_3 5%). These samples were digested in closed Teflon vessels until the temperature increase to 160 °C and maintained for 10 minutes. Then, the obtained solution was further digested with another mixture of acid (4 ml of HNO_3 65%, 4 ml of HCL 37% and 1 mL of HF 40%) until the temperature increased to 230 °C and maintained for 25 minutes. The final digested solution was then filtered through Whatman No.41 filter paper and stored in polyethylene bottles at 4°C until total metals composition analysis was conducted by inductively coupled plasma spectrometry (ICP).

3.1.4 Cation exchange capacity (CEC)

To determine CEC, the ammonium acetate method was used in this study (Department of Agriculture, 2010). Ammonium acetate solution (1 N, pH 7) was first employed to leach the samples. The samples were washed with ammonium chloride (0.25 N, pH 7) and 40% Ethanol. Subsequently, 10% sodium chloride was added to the samples to allow the exchange of ammonium ion. The amount of ammonium ion in the solution was investigated by distillation and titration with sulfuric acid as standard solution.

3.2 Synthesis of zeolite

Prior to the synthesis, the mixture of silica, aluminum, and sodium hydroxide (NaOH) was prepared. Either chemical aluminum (Al_2O_3) or aluminum dross was used as a main source of aluminum. On the contrary, CFA was applied to provide mainly silica and further supplement small amount of aluminum. Chemical

compositions of these raw materials were determined by XRF analysis. The suitable amount of aluminum dross/chemical aluminum and CFA required to obtain the target molar ratio was calculated. The ratio of silica to aluminum to NaOH of 1:1:1.2 was used during the synthesis of zeolite.

At the beginning, the homogenous mixture was fused in a furnace for 60 minutes at various temperatures including 550 °C, 600 °C, 700 °C, or 800 °C (CARBOLITE, AAF11/18/201). The fused product (20 g) was grinded and dissolved in 80 mL of deionized water and mixed by vigorous agitation using a reciprocal shaker (PNP, OS-3) at room temperature for 24 hours. Crystallization was performed under static condition for 12 hours followed by raising the temperature to 80 °C or 100 °C to obtain the product (Shaking water bath, GFL, 1086). The product was filtered, washed several times with deionized water, and dried at 100 °C for 12 hours (Oven, WTB Binder, FD115 (E2)).

3.3 Characterization of zeolite

In order to determine an optimal fusion temperature and crystallization temperature, CEC was investigated using ammonium acetate method. The crystalline structure and chemical composition of the obtained zeolite at optimum condition was analyzed using XRD and XRF. The morphology of the synthesized zeolite was analyzed using SEM, and BET was used to analyze the specific surface area (SSA).

3.4 Removal of cadmium by the synthesized zeolite

The adsorptive capability of the synthesized zeolites on cadmium was experimented. Preliminary experiment was conducted to establish suitable range of parameters for following experiments. The effect of contact time, and pH on cadmium removal was investigated. Subsequently, the adsorption of different initial concentrations of cadmium was studied, and the suitable isotherm was selected. If not specified otherwise, the initial pH was set at 5. Cadmium solution was prepared in water without buffering system since pH was not obviously affected during the experiment. However, in order to ensure no change pH, the pH at the end of the reaction was measured.

3.4.1 Preliminary experiment

The synthesized zeolite equivalent to 0.25, 0.5, or 1.0 g/L was weighted and added into an Erlenmeyer flask. Cadmium solution ($Cd(NO_3)_2$) at the concentration of 10 mg/L at pH 5 was prepared by added 1M NaOH, and 100 mL of this solution was transferred to the reaction. Mixing was provided by reciprocal shaking at 200 rpm (PNP, OS-3). Samples of cadmium solution were taken at 0, 5, 10, 20, 30, and 60 seconds after mixing the zeolite and cadmium solution. The samples were filtered through Whatman No.5 filter paper followed by adjusting the pH to less than 2 by

nitric acid. The obtained samples were analyzed by atomic absorption spectrophotometer (AAS, Analytik Jena, ZEEnit 700) to determine the concentration of cadmium. Reaction without the addition of zeolite was used as negative control.

3.4.2 Effect of contact time

The contact time required for zeolite to remove cadmium from the solution and reach its saturation point was investigated by extending the reaction time. A solution of 50 mg/L of cadmium was mixed with 0.25 g/L of each of the four synthesized zeolite samples by shaking at 200 rpm (PNP, OS-3). Samples were collected at 0, 5, 10, 20, 30, and 60 seconds, and 5, 10, 15, 30, and 60 minutes. Samples beyond 60 minutes were collected at 2, 3, 6, and 9 hours. After filtered through Whatman No.5 filter paper to remove the zeolite from the samples, pH of these samples was controlled to lower than 2 by nitric acid. Cadmium concentration of the samples was determined by AAS.

3.4.3 Effect of pH

Since the solubility of cadmium and structure of zeolite are pH dependent, the effect of pH on the adsorption efficiency of the synthesized zeolite was studied. The pH of 50 mg/L cadmium solution was adjusted to 2, 3, 4, 5, 6, 7, and 8 by 1M NaOH and 1M HNO_3. Subsequently, 100 mL of cadmium solution was mixed with 0.25 g/L of the synthesized zeolite by reciprocal shaking at 200 rpm (PNP, OS-3). Samples were collected at 3 hours after the adsorption started, and filtered by Whatman No.5 filter paper. The pH of the filtrate was controlled to less than 2 followed by AAS analysis to determine the concentration of cadmium.

3.4.4 Adsorption isotherm

The adsorption isotherm of the four synthesized zeolites (0.25 g/L) was determined by varying the initial cadmium concentration. The cadmium concentrations of 25, 35, 50, 75, 100, and 200 mg/L were prepared at pH 5. Samples of cadmium solution were taken at 3 hours after the mixing of zeolite and cadmium solution. The samples were filtered through Whatman No.5 filter paper followed by adjusting the pH to lower than 2. The obtained samples were then analyzed by AAS. The obtained data was then tested with three type of isotherms including linear, Langmuir, and Freundlich isotherms.

3.5 Removal of methylene blue (MB) by the synthesized zeolite

The sorption capacity of MB by the four synthesized zeolites was determined. MB was chosen for this study due to its widely used applications in many industries, especially in textile industrial, together with its potential adverse effect on health and the environment (Vargas et al., 2011). Suitable reaction time or contact time was

investigated, together with the adsorption of different initial concentrations of MB. Best fitted isotherm was then determined. The initial pH was set to 5. No additional pH control was applied during the experiments since pH was not obviously affected. However, the pH at the end of the experiments was tested to ensure no change pH.

3.5.1 Effect of contact time

Methylene blue removal by synthesized zeolite was conducted using the batch method. A solution of 50 mL of 10 mg/L of methylene blue solution was mixed with 0.025 g of the synthesized zeolites by shaking at 200 rpm (PNP, OS-3). Samples of methylene blue solution were taken at 15 and 30 minutes, and 1, 2, 3, 6, 9, 12, 24, 36, 48, 60, 72, 96, 120, 144, and 168 hours after mixing the zeolite with methylene blue solution. The collected samples were filtered through 0.45 μm membrane filter. The remaining concentrations of methylene blue in the obtained filtrates were investigated by UV/Vis Spectrophotometer (Thermo Electron Corporation, Helios Alpha) at the wavelength of 665 nm.

3.5.2 Adsorption isotherm

The adsorption of MB at various concentrations by the synthesized zeolites was examined in order to determine the adsorption isotherm. The initial methylene blue concentrations of 10, 30, 40, 50, 100, 200, and 300 mg/L were prepared. A solution of 50 mL at each concentration was mixed with 0.025 g of synthesized zeolites by shaking at 200 rpm (PNP, OS-3). After 120 hours, samples were filtered through 0.45 μm membrane filter and then determined the obtained samples by UV/Vis Spectrophotometer (Thermo Electron Corporation, Helios Alpha) (λmax = 665 nm). Data of MB concentration after treating with zeolites was applied to linear, Langmuir, and Freundlich isotherms to determined the best-fitted model.

CHAPTER IV

RESULTS AND DISCUSSIONS

4.1 Raw material analysis

4.1.1 Chemical compositions of CFA and aluminum dross

The chemical composition information of CFA and aluminum dross is shown in Table 4.1. The results indicated that the CFA used in this study consisted mainly of SiO_2 (78.71% by weight) and Al_2O_3 (9.57% by weight). It also contained small amount of other chemical components such as Fe_2O_3, P_2O_5, and CaO. In the case of aluminum dross, the major components were Al_2O_3 (48.04% by weight) and SiO_2 (8.58% by weight). A few other minor components were also detected including MgO, Fe_2O_3, and CaO. Since the collected CFA composed mainly of silica, it was used as a source of silica, whereas aluminum dross was utilized to provide additional aluminum due to its high aluminum content.

Based on the XRD analysis, the major crystalline phases in CFA were quartz and mullite together with some amorphous aluminosilicate glass components. In the case of aluminum dross, aluminum, aluminum oxide, aluminum nitride, and aluminum silicide were the major phases.

Table 4.1 Chemical composition of CFA and aluminum dross (XRF method)

Component (wt %)	CFA	Aluminum dross
SiO_2	78.71	8.58
Al_2O_3	9.57	48.04
Na_2O	0.02	0.37
Fe_2O_3	4.76	1.84
P_2O_5	2.49	0.19
CaO	2.14	1.65
MgO	0.027	3.70
TiO_2	0.88	0.56
K_2O	0.79	1.62
SO_3	0.15	0.46
BaO	0.09	0.11

4.1.2 Other raw material analyses

CFA and aluminum dross were identified from Notification of ministry of industry, BE 2548 to be Hazardous waste – Mirror entry (HM) and Hazardous waste – Absolute entry (HA), respectively. Concentration of total metal compositions of both CFA and aluminum dross were investigated to determine the metal content in the raw

material (Table 4.2). In the case of CFA, which is categorized as HM, the concentration of metals was compared to the standard Total Threshold Limit Concentration (TTLC) to determine whether CFA used in this study is toxic waste. The HM waste would be classified as toxic waste when metal concentration is equivalent or higher than indicated in TTLC. The obtained results revealed lower concentration of metals in CFA comparing to the TTLC; therefore, CFA in this study was not toxic waste. Some additional raw material characteristics were presented in Table 4.3.

Table 4.2 Total metal compositions of CFA and aluminum dross

Total metal compositions	Total concentration of raw materials (mg/kg)		TTLC (mg/kg) (Notification of ministry of industry, BE 2548)
	CFA	Aluminum dross	
Ag	2.26	3.05	500
Al	-	208555.04	-
B	-	160594.33	-
Ba	475.05	495.91	10,000
Bi	-	14.49	-
Ca	-	2584.99	-
Cd	19.16	5.90	100
Co	47.18	46.37	8,000
Cr	95.89	382.54	2,500
Cu	51.64	8287.75	2,500
Fe	-	7366.39	-
Ga	106.25	100.26	-
In	6.99	17.65	-
K	2034.5	5727.11	-
Li	85.15	3.51	-
Mg	920.13	4343.19	-
Mn	356.89	1935.59	-
Na	2356.45	3865.11	-
Ni	1730.70	670.23	2,000
Pb	28.48	278.40	1,000
Sr	442.99	54.27	-
Zn	97.55	3382.76	5,000

Table 4.3 other raw material analysis of CFA and aluminum dross

Parameters	Raw materials	
	CFA	Aluminum dross
pH	10.29	9.42
Moisture content (%)	0.11	-
LOI (%)	0.20	-
CEC (meq/100g)	8.00	-

4.2 Synthesis of zeolite

The zeolite samples obtained from different synthesis conditions were named as shown in Table 4.4.

Table 4.4 Sample code assignment

Sample	Source of Aluminum	Fusion Temperature (°C)	Boiling Temperature (°C)
P580	Aluminum oxide	550	80
P680	Aluminum oxide	600	80
P780	Aluminum oxide	700	80
P880	Aluminum oxide	800	80
P5100	Aluminum oxide	550	100
P6100	Aluminum oxide	600	100
P7100	Aluminum oxide	700	100
P8100	Aluminum oxide	800	100
D580	Aluminum dross	550	80
D680	Aluminum dross	600	80
D780	Aluminum dross	700	80
D880	Aluminum dross	800	80
D5100	Aluminum dross	550	100
D6100	Aluminum dross	600	100
D7100	Aluminum dross	700	100
D8100	Aluminum dross	800	100

4.2.1 Effect of fusion and crystallization temperatures

In this study, all of the zeolites were produced by heating the mixture of silicon, aluminum, and NaOH at high temperature. Two types of aluminum sources including aluminum oxide and aluminum dross were used together with CFA. Optimal condition of zeolite synthesis was determined by varying the fusion and crystallization temperature. Since several zeolite related applications involve ion exchange, efficiency of synthesis conditions were evaluated based on CEC value of the obtained products. The CEC values of the synthesized zeolites are illustrated in Figure 4.1.

4.2.1.1 Cation exchange capacity (CEC) of the synthesized zeolites

In the case of aluminum oxide, the highest CEC value was found corresponding to the fusion temperature at 700 °C with crystallization temperature at 80 °C. Zeolites obtained from 80 °C of crystallization consistently exhibited relatively higher CEC comparing to those generated at 100 °C. In terms of the optimal fusion temperature, highest CEC among the synthesized zeolites generated from the same set of crystallization temperature was observed at 700 °C in both crystallization temperatures.

On the other hand, the highest CEC of the synthetic zeolite using aluminum dross was detected at 600 ˚C and 80˚C of fusion and crystallization temperatures, respectively. As the overall effect of crystallization temperature, most of the zeolites produced under fusion temperature at 600 ˚C and 700 ˚C showed higher CEC when crystallization was allowed at 80 ˚C. Interestingly, at 550 ˚C fusion temperature, more than two times higher in CEC was detected in zeolites obtained from crystallization at 100 ˚C. As for the influence of fusion temperature on the CEC value, zeolites synthesized from two crystallization temperatures exhibited different optimal fusion temperature. At 80 ˚C, highest CEC value was observed in samples generated at 600 ˚C fusion temperature, whereas, at 100 ˚C, optimal fusion temperature was found to be 550 ˚C. This suggests that different fusion and crystallization temperature may have combinatory effect on the obtained zeolites.

Collectively, most of the CEC values of the synthesized zeolite using aluminum oxide, except sample from 550˚C fusion and temperature and 100 ˚C crystallization temperature, are higher than those of synthesized zeolite using aluminum dross. This may result from the impurity of aluminum dross, which has lower purity comparing to the chemical grade aluminum oxide.

All CEC values of the synthesized zeolite using aluminum oxide or aluminum dross were compared with CEC value of commercial zeolite 4A obtained from a study conducted by Font er al. (2009). According to the reference, zeolte 4A was supplied by IQE S.A (Industrias Químicas del Ebro), and the CEC value of this commercial zeolite 4A was 540 meq/100g (Font et al., 2009). All of the zeolites produced in this study exhibited lower CEC comparing to the commercial zeolite.
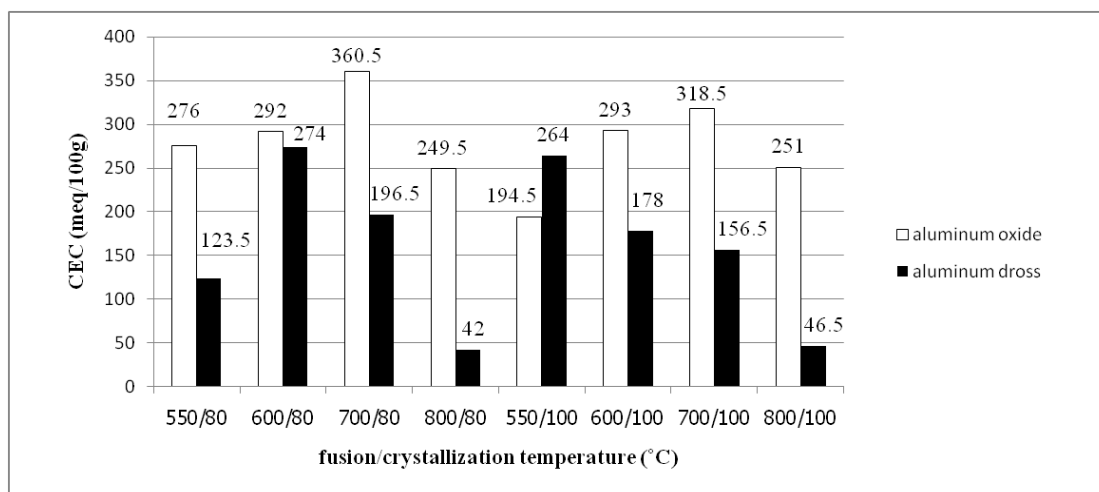
Figure 4.1 Effect of fusion and crystallization temperature on the CEC value of the synthesized zeolite obtained using two kinds of aluminum

4.2.1.2 Crystalline structure of the synthesized zeolites

It is well known that the alkali fusion method is crucial for complete decomposition of the quartz and mullite (Berkgaut and Singer, 1996; Kazemian et al., 2010), which serve as sources of silicon and aluminum. The process first generates some chemical species including sodium silicate (Shigemoto et al., 1993; Chang and Shih, 2000; Yaping et al., 2008; Kazemian et al., 2010), sodium aluminate (Shigemoto et al., 1993; Berkgaut and Singer, 1996; Chang and Shih, 2000), sodium metasilicate (Berkgaut and Singer, 1996), and sodium aluminosilicate (Berkgaut and Singer, 1996; Yaping et al., 2008), which are generally more dissolvable than quartz and mullite themselves. However, after the alkaline fusion process certain chemical residues may remain, and types of the generated zeolite may be varied. Therefore, the crystalline structure of the synthesized zeolites was examined by XRD to ensure desire zeolite type with limited unintended chemical residues.

The XRD results of the zeolites synthesized from different types of aluminum are shown in Figure 4.2 to 4.5. In this study, only type A zeolite was generated in this study. When the aluminum oxide was used together with crystallization temperature at 80 ˚C (Figure 4.2), zeolite A with no remaining residues of other chemical species was detected. Similarly, at 100 ˚C crystallization temperature (Figure 4.3), XRD analysis of the obtained products at all fusion temperatures except at 550 ˚C revealed existence of zeolite A without other residues. Nonetheless, certain remaining residues were observed in the product from 550 ˚C fusion temperature.

For those products resulting from the addition of aluminum dross into fusion process, zeolite A was detected in most samples; however, many synthesis conditions sodium aluminum silicate and other chemical residues remain. At 80 ˚C crystallization temperature (Figure 4.4), fusion temperature at 600 ˚C produced only zeolite A, whereas both zeolite A and sodium aluminum silicate were detected at 550 and 700 ˚C. Fusion temperature at 800 ˚C generated only sodium aluminum silicate with no zeolite product. Although sodium aluminum silicate was detected at 550, 700, and 800 ˚C, zeolite A without other residues was generated at 600 ˚C.

In the case of 100 ˚C crystallization temperature (Figure 4.5), zeolite A and some remaining residues were found at 550, 600, and 700 ˚C fusion temperature. Similarly to 80 ˚C crystallization temperature and 800 ˚C fusion temperature, which observed only sodium aluminum silicate, at 100 ˚C crystallization temperature with 800 ˚C fusion temperature mainly sodium aluminum silicate was detected but with trace amount of zeolite A. Although most of the samples from aluminum dross contained other residues beside zeolite A, the results of 80 ˚C crystallization temperature with 600 ˚C fusion temperature indicated that at a suitable condition, the production of zeolite was not negatively affected by the addition of aluminum dross. Furthermore, the CEC

value of samples obtained from this condition was highest among all the conditions examined with aluminum dross.
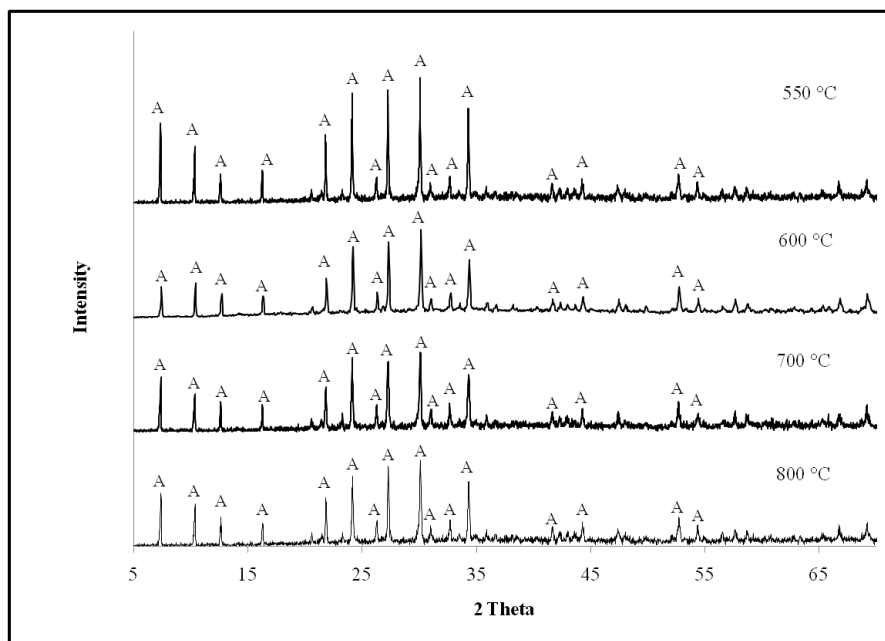
Figure 4.2 XRD patterns of synthesized zeolite using aluminum oxide at different fusion temperature; M = mullite, Q = quartz, A = zeolite A (crystallization temperature at 80 ˚C)
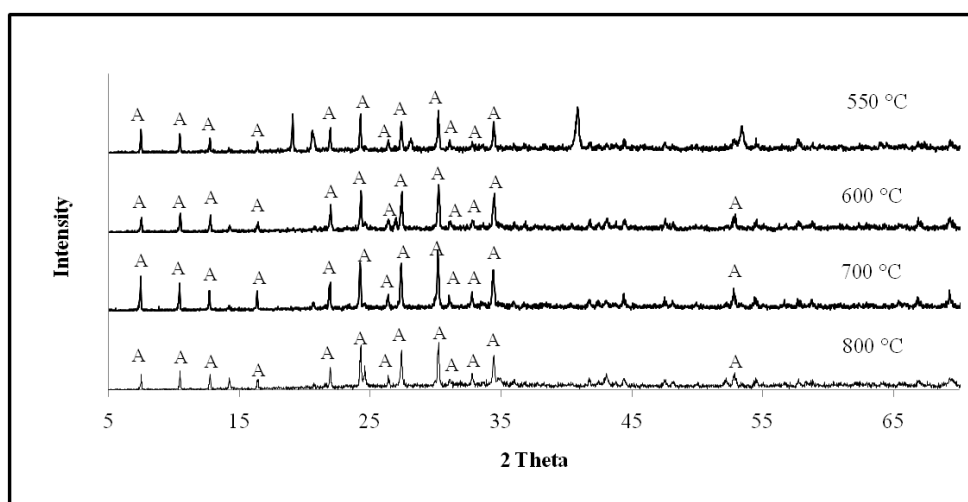
Figure 4.3 XRD patterns of synthesized zeolite using aluminum oxide at different fusion temperature; M = mullite, Q = quartz, A = zeolite A (crystallization temperature at 100 ˚C)
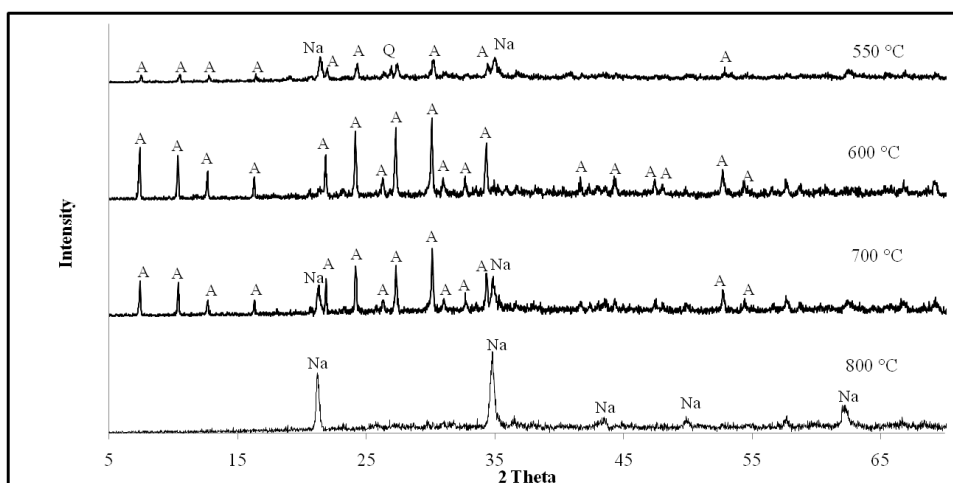
Figure 4.4 XRD patterns of synthesized zeolite using aluminum dross at different fusion temperature; M = mullite, Q = quartz, A = zeolite A, Na = sodium aluminum silicate (crystallization temperature at 80 ˚C)
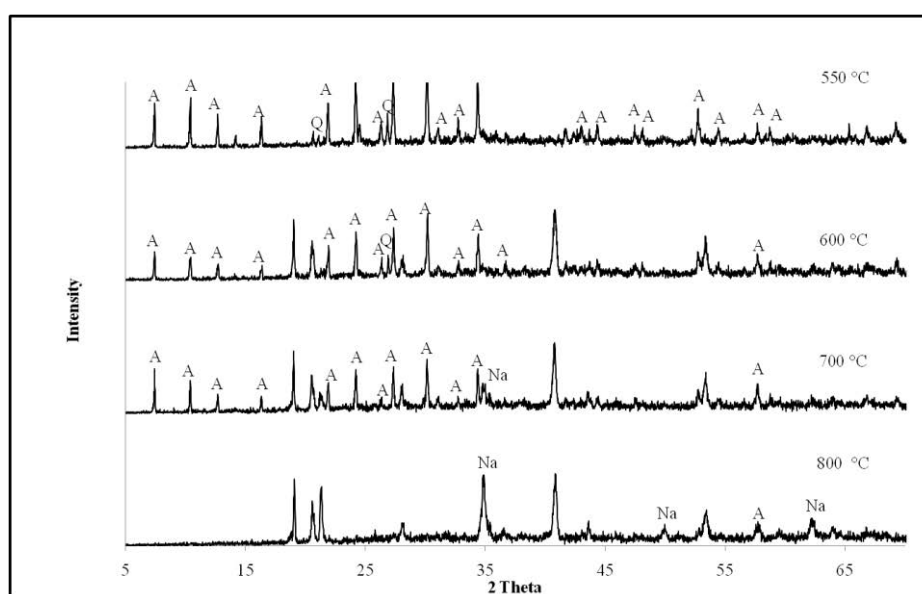
Figure 4.5 XRD patterns of synthesized zeolite using aluminum dross at different fusion temperature; M = mullite, Q = quartz, A = zeolite A, Na = sodium aluminum silicate (crystallization temperature at 100 ˚C)

Four samples were selected for further analyses and experiments; (1) zeolite synthesized at 600 ˚C using aluminum oxide (P680), (2) zeolite synthesized at 700 ˚C using aluminum oxide (P780), (3) zeolite synthesized at 600 ˚C using aluminum dross (D680), and (4) zeolite synthesized at 700 ˚C using aluminum dross (D780). Both P780 and D680 are samples that exhibited the highest CEC among the samples synthesized using aluminum oxide and aluminum dross, respectively. In addition, the samples from the same synthesis condition, but different types of aluminum (P680 and D780), were selected for sample comparison.

4.3 Characterization of synthesized zeolite

4.3.1 X-ray fluorescence analysis

The chemical composition of the four selected samples was analyzed by XRF, and the results are shown in Table 4.5. Among the synthesized products, the ratio of SiO_2 to Al_2O_3 ranged from 1.27 to 1.54 which is similar to the ratio obtained from the commercial zeolite A (Purna Chandra Rao et al., 2006). Moreover, according to the morphology determined by SEM and crystalline structure analyzed by XRD, consistent results suggested that the synthesized products zeolite A.

Table 4.5 Chemical composition of selected zeolite samples

Samples	%SiO_2	%Al_2O_3	SiO_2/Al_2O_3
P680	27.18	19.32	1.41
P780	31.64	20.54	1.54
D680	27.44	18.51	1.48
D780	38.02	30.00	1.27
Zeolite 4A (commercial grade) (Purna Chandra Rao et al., 2006)*	34.12	28.30	1.21

* Zeolite 4A (Purna Chandra Rao et al., 2006) is a commercial grade zeolite from Indian Petro Chemicals Limited, Vadodara, India. Particle size and pore diameter of this zeolite4A are 3-8 µm and 4 angstrom, respectively.

4.3.2 Morphology

The SEM images of D680, D780, P680 and P780 are shown in Figure 4.6. The images revealed the morphology of the synthesized samples which is mainly cubic-like structure. This suggests that the synthesized products are zeolite A since this type of zeolite normally exhibits a cubic-like morphology.
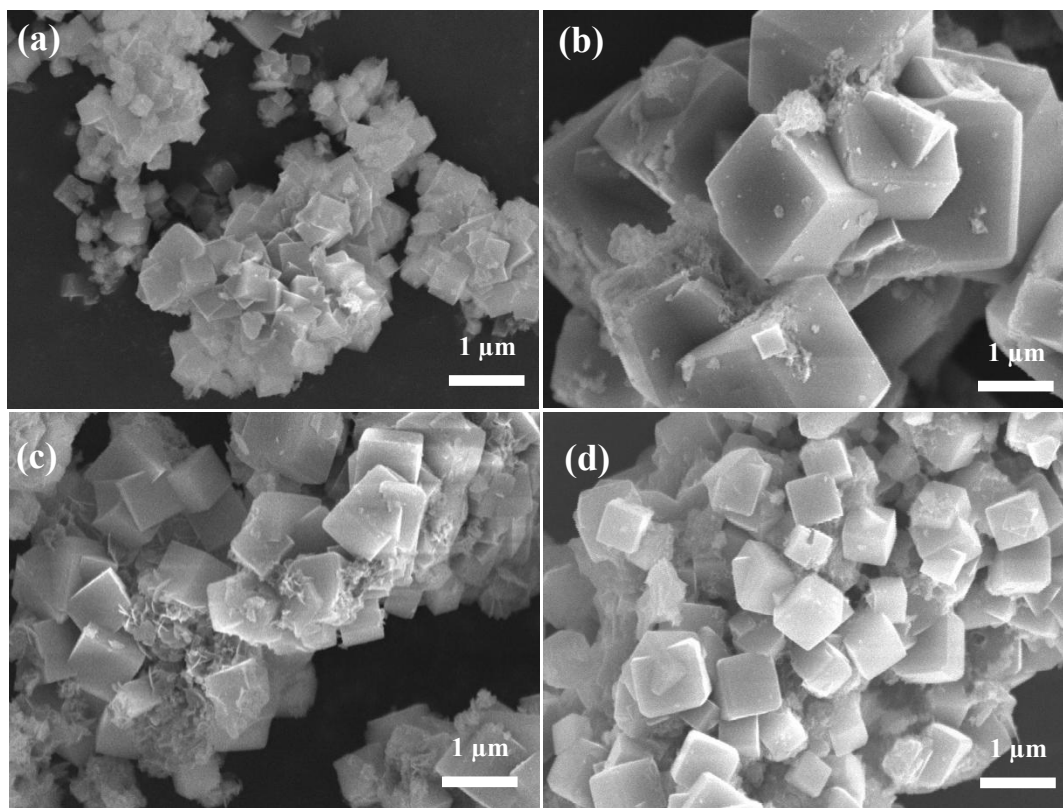
Figure 4.6 SEM analysis of (a) P680 (b) P780 (c) D680, and (d) D780

4.3.3 Specific Surface Area (SSA)

Specific surface area (SSA) of the four zeolite samples were determined and presented in Table 4.6. Interestingly, between samples synthesized from the same type of aluminum, the SSA of sample obtained from 700 ˚C fusion temperature was slightly higher than the one produced from 600 ˚C. The higher SSA of P680 compared to D680, and P780 compared to D780, was consistent with the SEM results in which the samples synthesized using dross as aluminum source exhibited larger particle size.

Table 4.6 Specific surface area of the synthesized zeolite

Samples	SSA (m^2/g)
P680	20.76
P780	23.46
D680	18.80
D780	21.34
Zeolite 4A (commercial grade) (Purna Chandra Rao et al., 2006)	655

4.4 Removal of cadmium by the synthesized zeolite

The adsorption process can be affected by various parameters such as contact time, pH, and concentration of cadmium solution. Therefore, the effect of these parameters on the cadmium of cadmium was investigated to optimize the adsorption process.

4.4.1 Preliminary experiment

Prior to the investigation of the effects of different parameters on the adsorption efficiency, preliminary experiments were conducted to establish range of initial condition for further experiments. The adsorption of cadmium using different concentrations of zeolite was investigated (Figure 4.7). At 10 mg/L of cadmium, less than 1 mg/L of cadmium (more than 90% removal) was detected after 5 seconds of adsorption suggesting a high adsorption efficiency of the synthesized zeolite.

No difference in terms of total adsorption was observed among zeolite samples synthesized by the four different conditions. This might due to the high adsorption capacity and removal rate of the synthesized zeolite in which more than 90% of total cadmium in the solution was adsorbed in all concentration of zeolite used (0.25, 0.5, and 1 g/L). The control in which zeolite was excluded from the reaction showed no decrease in cadmium concentration.

Since rapid cadmium removal was observed in all three zeolite concentrations, the lowest concentration (0.25 mg/L) of zeolite was chosen for the next experiment together with the increment of cadmium concentration.
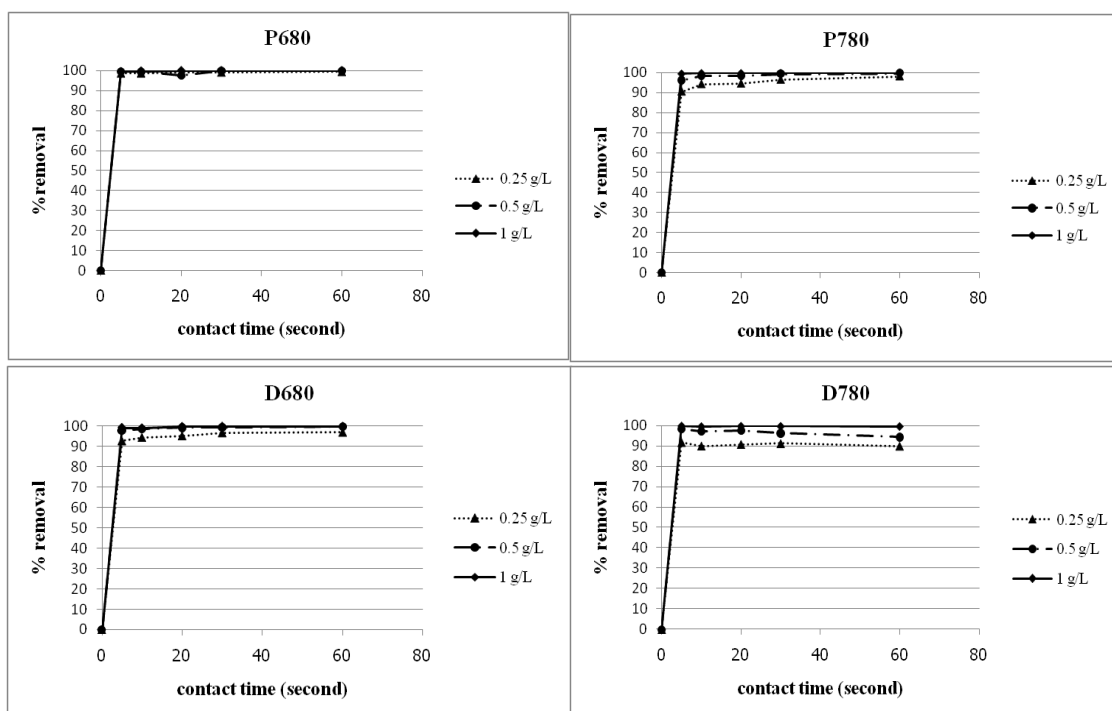
Figure 4.7 Removal of 10 mg/L cadmium at zeolite/cadmium ratio of 0.25, 0.5, and 1 g/L for P680, P780, D680, and D780

4.4.2 Effect of contact time

In order to study the adsorption capacity of the synthesized zeolite and contact time required for total adsorption, cadmium concentration was increased to 50 mg/L. Results indicated that, after 5 minutes, about 34.68 mg/L of cadmium (70%) was removed from the solution by 0.25 g/L of D680 (Figure 4.8). The detectable cadmium became less than 5 mg/L (about 91% removal) after 3 hours of adsorption by D680. The adsorption by P780, which exhibited about 89% removal of cadmium in 3 hours, was slightly lower than adsorption by D680. In contrary to D680 and P780, P680 and D780 showed relatively lower adsorption efficiency, which might result from suboptimum synthesis conditions according to the low CEC and SSA of the synthesized products (P680 and D780). No decrease in cadmium concentration was observed in control reactions lacking of the synthesized zeolite.

Among these 4 zeolite samples, D780 exhibited lowest cadmium adsorption (about 77% removal of cadmium after 3 hours). The high adsorption of P780 was consistent with the CEC and SSA data in which highest CEC and SSA were found in P780. Interestingly, D680 exhibited highest adsorption although D680 showed relatively low CEC and SSA comparing to other synthesized zeolite samples in this study. The high cadmium adsorption by D680 suggests that aluminum dross may be used instead of chemical aluminum for the synthesis of zeolite without negatively

affecting its adsorption capacity and rate. . The contact time of 3 hours was selected for the next experiment since only limited increase in cadmium removal was observed after this period.
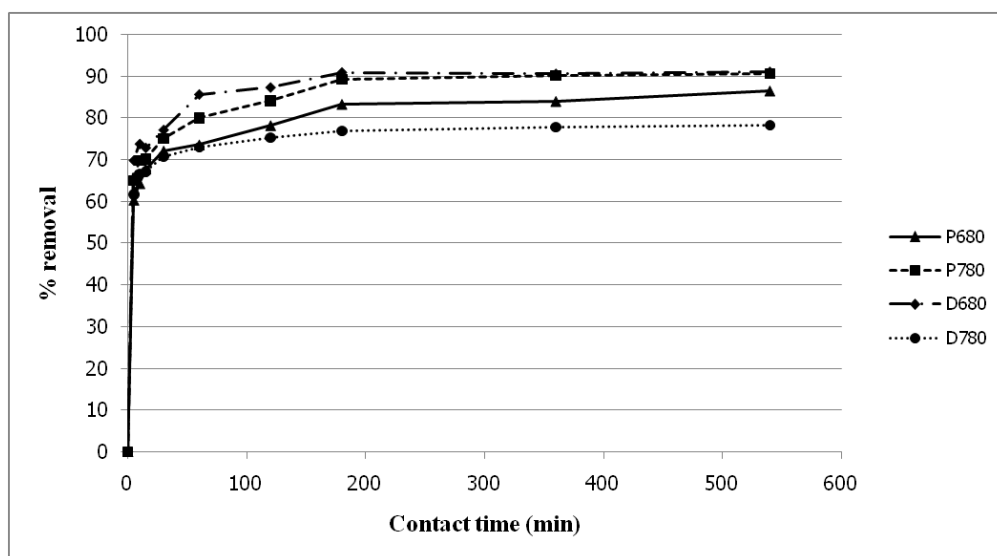
Figure 4.8 Effect of contact time of P680, P780, D680, and D780 (initial concentration of cadmium of 50 mg/L, zeolite dose 0.25 g/L, pH = 5)

4.4.3 Effect of pH

In order to determine whether the pH may affect the solubility of cadmium was investigated as shown in Figure 4.9. The experiment was conducted at room temerature. The cadmium concentration in the solution was measured without addition of zeolite. At pH 2 to 5, the observed cadmium concentration was more than 40 mg/L, whereas the detectable cadmium concentration became lower (35.45 mg/L) once the pH was elevated to 6. At pH 7, the concentration of cadmium was lowered to 23.75 mg/L. This revealed that the solubility of cadmium is crucially affected and decreased when the pH of the solution increased to 6.

The effect of pH on the adsorption of cadmium by zeolite was investigated and the results were shown in Figure 4.10. In order to exclude the effect of pH on the solubility of cadmium, the percent removal of cadmium was calculated based on cadmium concentrations after precipitation at different pH as initial concentrations. All experiments were conducted under room temperature. The results showed that the removal of cadmium in the solution is dependent on the pH of the solution. The adsorption of cadmium increased with increasing pH of solution in all of the adsorbents. Low removal of cadmium in the solution was observed at low pH such as 2 and 3. Hydrogen ions may affect the adsorption of cadmium by competing binding to zeolite. In the zeolite with low Si/Al ratios such as zeolite A, Si-O-Al is more easily

damaged than Si-O-Si and can be easily attached by hydrogen ions (Purna Chandra Rao et al., 2006). The higher adsorption was observed as the pH increased. At pH 4 more than 80% cadmium removal was observed in both P780 and D680. At pH 5 and 6 more than 80% cadmium removal was observed in P680, P780 and D680, respectively. At pH 7 and 8 more than 90% cadmium removal was observed all of synthesized zeolites (P680, P780, D680, and D780). The sorption capacity of the four synthesized zeolites at different pH was presented in Figure 4.11. Extremely lower sorption capacity was observed at low pH such as 2. The sorption capacity was then increased along with the elevated pH used. This trend continued until the pH was around 4 and 5. Dramatic decrease in sorption capacity was detected once the pH was higher than 5. Highest sorption capacity of P680, P780, and D680 was found at pH 5, whereas the highest sorption for D780 was observed at pH 4. Therefore, pH 5 was selected for further studies since high adsorption capacity was detected and since pH lower than 4 should be avoided for the adsorption by zeolites (Purna Chandra Rao et al., 2006). From the obtained results, pH 5 was chosen for further experiments to avoid cadmium precipitation at high pH and low adsorption efficiency at low pH.
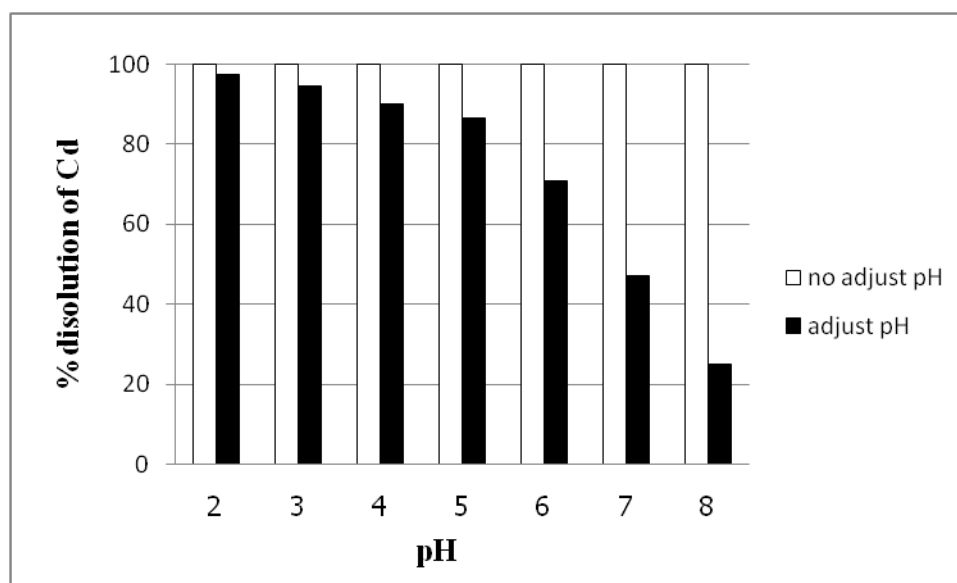
Figure 4.9 Relationship between pH and dissolution of 50 mg/L cadmium of without the zeolite
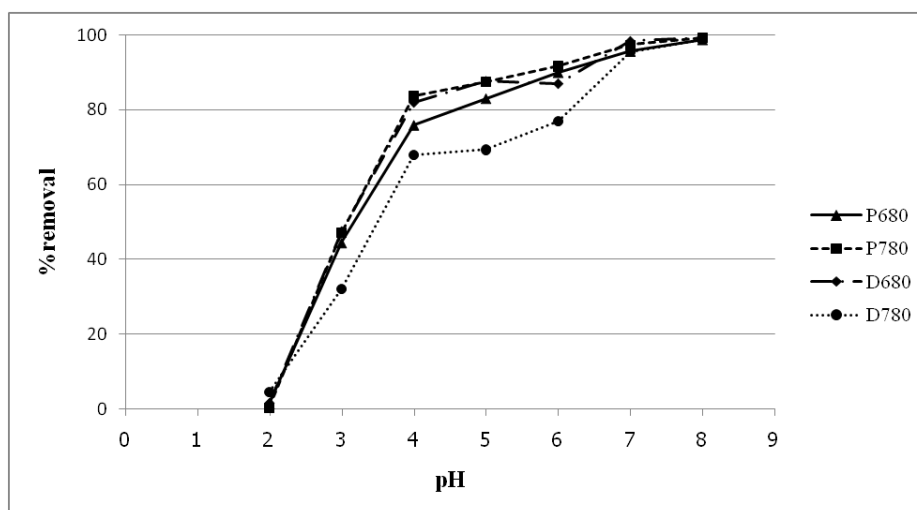
Figure 4.10 Effect of initial pH on the synthesized zeolites (P680, P780, D680, and D780)
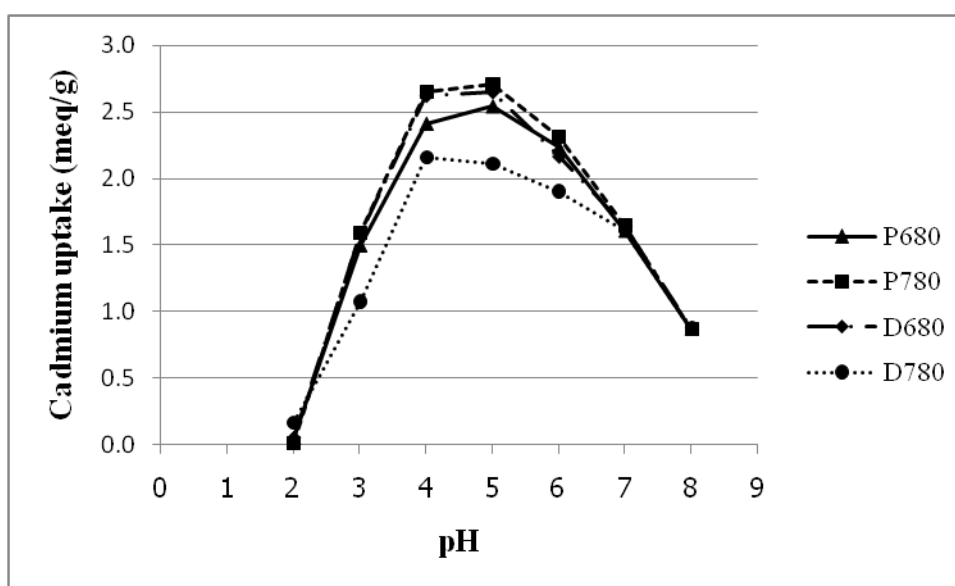
Figure 4.11 Effect of pH on cadmium uptake of synthesized zeolites (P680, P780, D680, and D780)

4.4.4 Effect of initial concentration of cadmium

The effect of initial concentration of cadmium was investigated among the four samples of zeolites (Figure 4.11 and 4.12). Cadmium removal efficiency of P680 at 25 mg/L cadmium was 99.40% which accounted for 89.22 mg/g adsorption capacity. Cadmium removal at 200 mg/L cadmium decreased to 25.22%. Interestingly, although the removal percentage was lower, adsorption capacity of P680 increased to 195.41 mg/g. Similarly, cadmium removal of P780 at 25 mg/L and 200 mg/L cadmium was 99.76% and 23.94%, respectively, whereas the capacity

increased from 89.55 mg/g to 187.00 mg/g. In the case of D680, removal was 99.75% at 25 mg/L of cadmium, and reduced to 24.84% at 200 mg/L of cadmium. On the other hand, adsorption capacity increased from 89.54 mg/g to 192.46 mg/g. Percent removal of D780 reduced from 99.33% at 25 mg/L cadmium to 21.71% at 200 mg/L cadmium, when sorption capacity increased from 89.51 mg/g to 168.93 mg/g.

The results were also presented in the form total adsorption (Figure 4.13). Although the removal percentage at high initial cadmium concentrations was realatively lower comparing to those in lower initial concentrations, sorption increased along with elevated initial cadmium concentrations. At 25 mg/L of cadmium, about 1.5 meq/g of sorption was observed among the four types of zeolites. For most of the zeolites, the sorption increased to about 3 meq/g at 100 mg/L of initial concentration of cadmium where the removal percentage was lower to less than 50 %. The highest sorption capacity in this study was observed in the range of 3.5 to 3.4 meq/g at 200 mg/L of cadmium initial concentration from P680, P780 and D680. This was consistent with high CEC value observed among these samples.

The adsorption capacity of the aluminum dross based zeolite (D680) was comparable to those synthesized from chemical grade aluminum oxide, hence revealed the possibility of using this dross in zeolite production. However, P780 exhibited both lower removal percentage and adsorption capacity which was consistent with its CEC result, which was lower than P680, P780 and D680.

All these results revealed that at a lower cadmium concentration, the percent removal of cadmium was high, and gradually decrease along with the increasing cadmium concentration. This may due to limited space of zeolites since more binding spaces are required when more cadmium is available. In contrast to the cadmium removal percentage, sorption capacity of the sorbent tended to increase along with the increase in cadmium concentration. This may result from the increased in transfer driving force when the concentration become higher (Jain and Ram, 1997; Jamali et al., 2009).

Although only one species of heavy metals was tested in this study, more than one species of metal species may be found together in a typical water treatment system or contaminated site. Previous study indicated that having different metal species in the same system may affect the sorption efficiency and the removal of each species may be varied depending on the combination of metal species (Hui et al., 2005). Thus, more tests are required in order to evaluate the potential uses of the synthesized zeolites in this study.

Figure 4.12 Effect of intial cadmium concentration on the removal of cadmium by P680, P780, D680, and D780 (sample dose = 0.25 g/L, initial pH = 5)

Figure 4.13 Effect of intial cadmium concentration on the sorption capacity by P680, P780, D680, and D780 (sample dose = 0.25 g/L, initial pH = 5)

4.4.5 Adsorption isotherm

The linear regression and Langmuir and Freundlich isotherm models were depicted in Figure 4.13, 4.14, and 4.15, respectively. The fitted constants and regression coefficients for the linear, Langmuir, and Freundlich models were summarized in Table 4.7 and 4.8. According to the regression coefficients (R^2) of the synthesized zeolites, the cadmium adsorption was best fitted with Freundlich isotherm comparing among the three models. This suggests that the cadmium adsorption by the synthesized zeolites occurred in a heterogeneous system. The adsorption reaction was reversible and multilayer together with different level of adsorption energy (El Qada et al., 2006). The constants K_F (adsorption capacity) and n (degree of non-linearity) were calculated and shown in Table 4.8. The values of the heterogeneity factor (1/n) in Table 4.8 indicated that all samples zeolite have a heterogeneous structure. Furthermore, the 1/n of all samples that were less than 1 suggested that the adsorption was slightly suppressed at lower concentrations of cadmium. The values of n indicate whether the adsorption is linear regression (n=1), favorable by chemical process (n<1), or favorable by physical process (n>1) (Vargas et al., 2011). The values of P680, P780, D680, and D780 were 9.31, 10.80, 10.78, and 11.99, respectively. This revealed that cadmium is favorably adsorbed by all samples via physical process. The K_F also indicated that P780 has the highest cadmium removal following by D680, P680, and D780, respectively. This was in concert with the CEC, which can be arranged in the following order from high to low: P780 > P680 > D680 > D780.

Figure 4.14 Linear regression for the adsorption of synthesized zeolites (P680, P780, D680, and D780)

Figure 4.15 Langmuir isotherm for the adsorption of synthesized zeolites (P680, P780, D680, and D780)

Figure 4.16 Freundlich isotherm for the adsorption of synthesized zeolites (P680, P780, D680, and D780)

Table 4.7 Equations and regression coefficient (R^2) for Linear regression and Langmuir and Freundlich isotherm

Materials	Linear regression		Langmuir isotherm		Freundlich isotherm	
	equation	R^2	equation	R^2	equation	R^2
P680	y=0.5557x+122.08	0.718	y=0.0007x+0.0065	0.793	y=0.1074x+2.0445	0.986
P780	y=0.4561x+129.39	0.539	y=0.0003x+0.0064	0.827	y=0.0926x+2.0808	0.981
D680	y=0.4969x+127.54	0.607	y=0.0003x+0.0064	0.825	y=0.0928x+2.0798	0.978
D780	y=0.4517x+103.45	0.880	y=0.0005x+0.0079	0.545	y=0.0834x+1.991	0.840

Table 4.8 Constant value for Linear regression and Langmuir and Freundlich isotherm

Materials	Linear regression	Langmuir isotherm		Freundlich isotherm	
	K_d	q_{max} (mg/g)	b (l/g)	K_F (mg/g)	1/n
P680	0.556	153.85	9.29	110.79	0.1074
P780	0.456	156.25	21.33	120.45	0.0926
D680	0.497	156.25	21.33	120.17	0.0928
D780	0.452	126.58	15.80	97.95	0.0834

4.5 Removal of methylene blue (MB) by the synthesized zeolites

4.5.1 Effect of contact time

The adsorptions of methylene blue in all of the four synthesized zeolite samples were increased along with the reaction time. High adsorption rate was observed in P780 samples; with more than 60% of total methylene blue was adsorbed within about 30 minutes after the reaction started. The adsorption of methylene blue by P780 quickly reached its saturation after 36 hours of the reaction. For P680, D680, and D780, about 40% of methylene blue adsorption was observed after the adsorption reaction was carried out for 1 hour. No obvious adsorption was detected after 72 hours. However, a very slight increase in the sorption (less than 1-2%) was observed until 120 hours. Therefore, a 120 hours contact time was selected as equilibrium time point for further study. Total adsorption of methylene blue by D780, P780, P680, and D680 were 84.21%, 80.70%, 79.18%, and 70.18%, at 120 hours respectively. Interestingly, the adsorption of methylene blue using zeolite synthesized from aluminum dross (D780) showed a promising potential according to the highest total adsorption observed in this sample. On the contrary, the D680 exhibited much less adsoprtion efficiency when compared to other zeolite samples. This suggests that the synthesis conditions may have an important role in dictating the characteristics of these zeolite products.
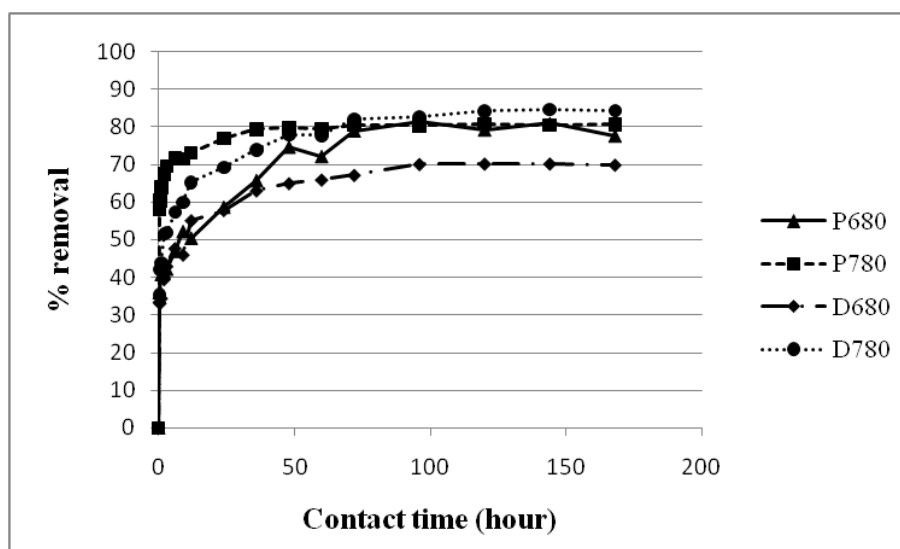
Figure 4.17 Effect of contact time on P680, P780, D680, and D780 samples

4.5.2 Effect of initial concentration of methylene blue (MB)

The effect of initial MB concentration on its total removal and removal capacity of the synthesized zeolites was investigated and presented in Figure 4.17 and 4.18, respectively. Various concentrations ranging from 10 mg/L to 300 mg/L of MB were used, and the observed MB removal was gradually lowered along with the increasing initial concentration. From 10 mg/L to 300 mg/L of MB, MB removal by P680 reduced from 73.08% to 9.65%. Similarly, the observed MB removal of P780 was reduced from 71.26% to 7.81 %. MB removal of D680 and D780 were lowered from 64.7% to 8.53% and from 83.32% to 12.28 %, respectively.

In contrast, increase in MB adsorption of all zeolites generated from different conditions was detected when higher initial MB concentrations were applied. The sorption of P680 and P780 increased from 15.19 mg/g to 63.67 mg/g and from 14.57 mg/g 51.77 mg/g, respectively. Higher sorption was also observed in D680 (13.39 mg/g to 56.30 mg/g) as well as in D780 (17.25 mg/g to 81.03 mg/g). Therefore, even though the percent removal decreased under high initial MB concentrations, the removal of MB was actually increased.

The removal capacity of the four synthesized zeolites in term of meq/g of zeolite was calculated and shown in Figure 4.18. Similarly to the total removal of MB, the adsorption increased along with the higher initial concentrations of MB. However, when comparing the sorption capacity at the sautration point between cadmium and MB using the same batch of zeolites, the highest ion exchange capacity in the case of cadmium was higher (3.5 meq/g) than that of MB (0.25 meq/g) by the zeolites was more. This suggests that ion exchange may not be the main removal mechanism of MB by the synthesized zeolites.

Collectively, when higher initial MB concentration was applied, the removal of MB became lower. Interestingly, with the lower overall removal, the sorption capacity of the synthesized zeolites was increased. These observations were similar to those found in cadmium adsorption, thus same explanation may be applied. Lower removal percentage may resulted from the limited space for the adsorption to occur once all the free space was filled, whereas the increased sorption capacity may due to the elevated transfer driving force under high concentration of MB.
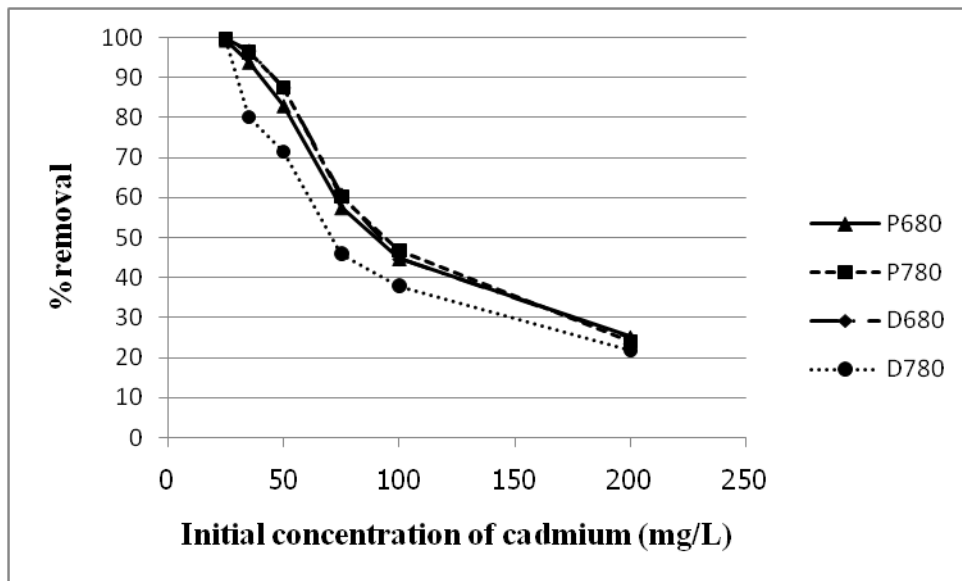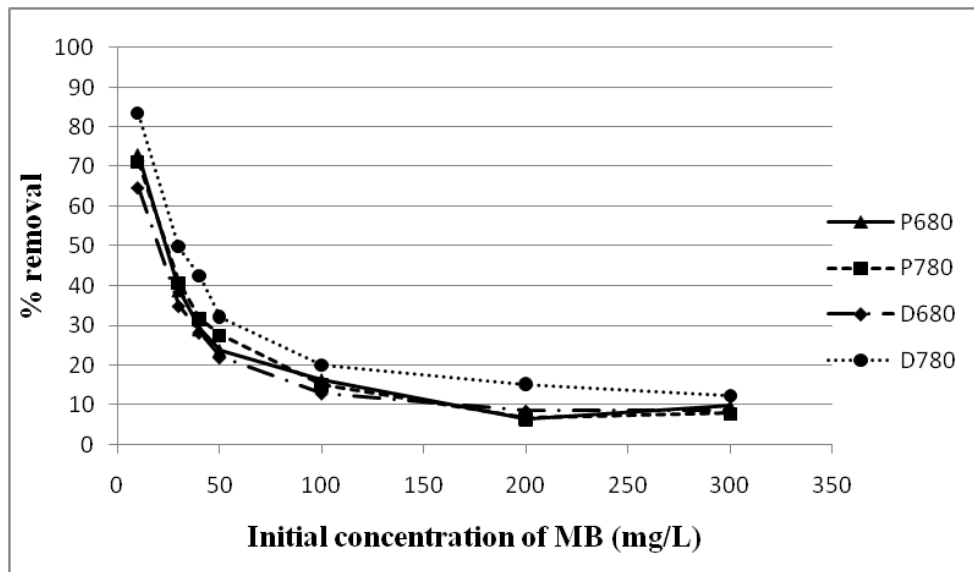
Figure 4.18 Effect of initial MB concentration on the removal of MB by P680, P780, D680, and D780 (sample dose = 0.5 g/L, contact time = 5 days)
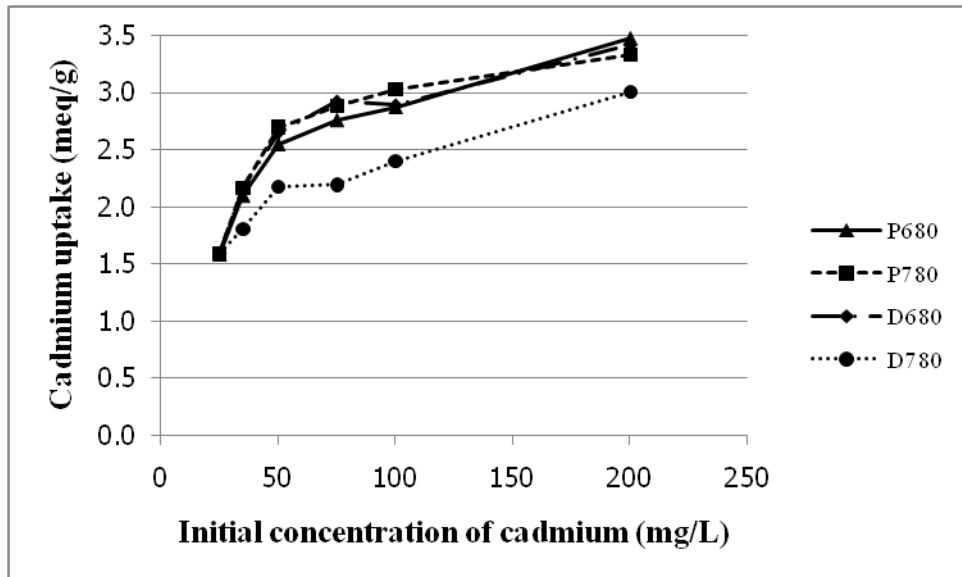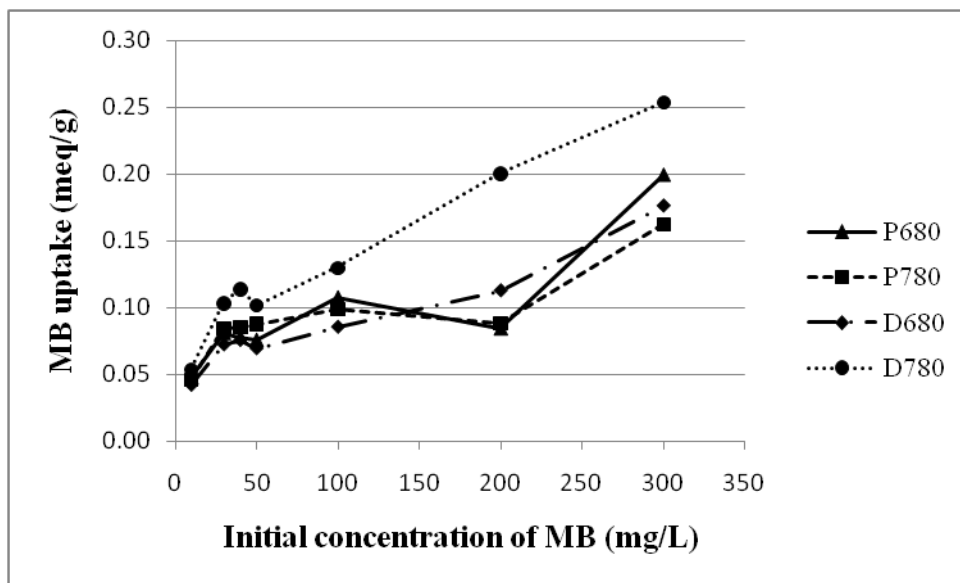

Figure 4.19 Effect of intial MB concentration on the sorption capacity by P680, P780, D680, and D780 (sample dose = 0.5 g/L, contact time = 5 days)

4.5.3 Adsorption isotherm

Linear regression and Langmuir, and Freundlich isotherms were applied to the obtained MB adsorption results and illustrated in Figure 4.19, 4.20, and 4.21, respectively. Although the MB adsorption could not be fitted with any of these models, among these three models, the adsorption behavior of D780 and D680 were best explained by the Freundlich isotherm, which suggested a heterogeneous system. All of the four synthesized zeolite samples exhibited heterogenous factor (1/n) that was lower than one. This suggests that these zeolites have heterogeneous surface structure and are subjected to only limited suppression at low concentration of adsorbate.

Interestingly, the K_F of the synthesized zeolites from aluminum dross was higher than those from aluminum oxide based zeolites. This suggests that zeolites from aluminum dross may provide even better adsorption of MB. However, this was contradict to the CEC value of the zeolite sample in which high CEC was observed in aluminum oxide derived zeolite (P780). Therefore, the main sorption mechanism of MB may not be ion exchange. Rather than the ion exchange mechanism, the main adsorption mechanism might rely mostly on surface adsorption since the high adsorption capacity was observed in zeolites with high SSA but low CEC (D780). This is consistent with the previous that indicated important role of surface area in the adsorption of MB (Wang et al., 2006). Beside cation exchange with MB in the form of MB+, physical adsoprtion involving the sorption of MB on the zeolite surface, boundary layer of adsorbent, other active sites, and interior pourous structure of zeolites (Doğan et al., 2009; Rafatullah et al., 2010). However, in this study, the main purpose was to investigate the application of the synthesized zeolite involve mainly in cation exchange.
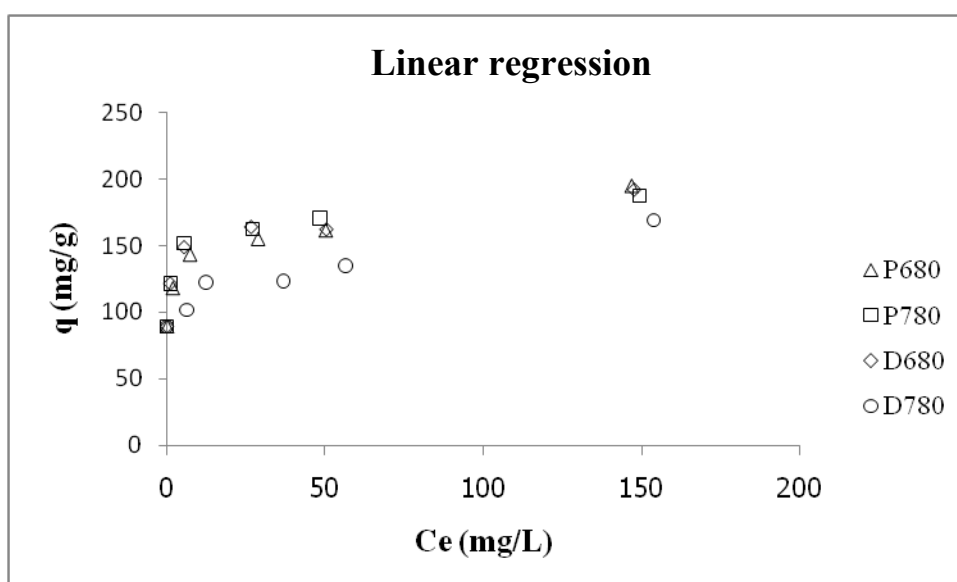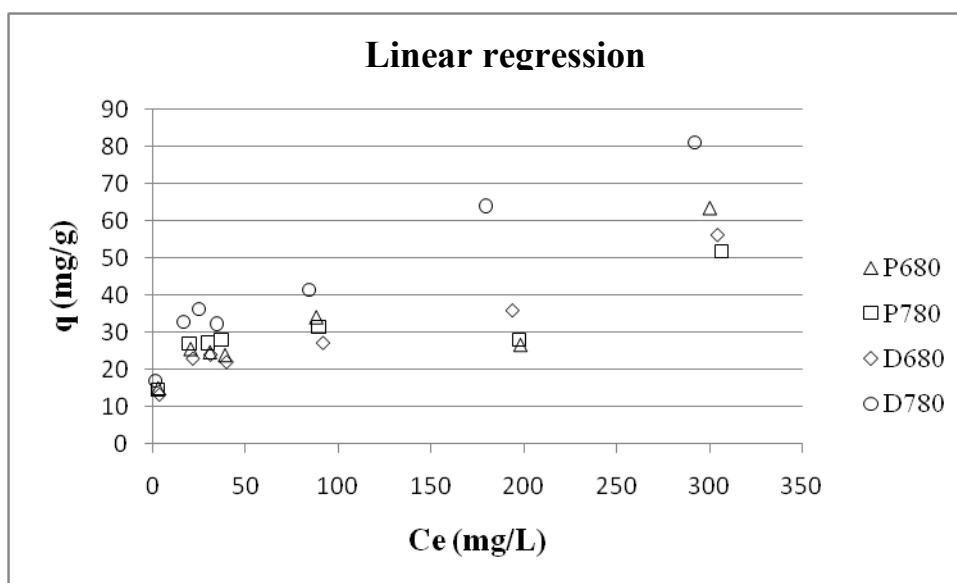
Figure 4.20 Linear regression for the adsorption of MB by synthesized zeolites (P680, P780, D680, and D780)
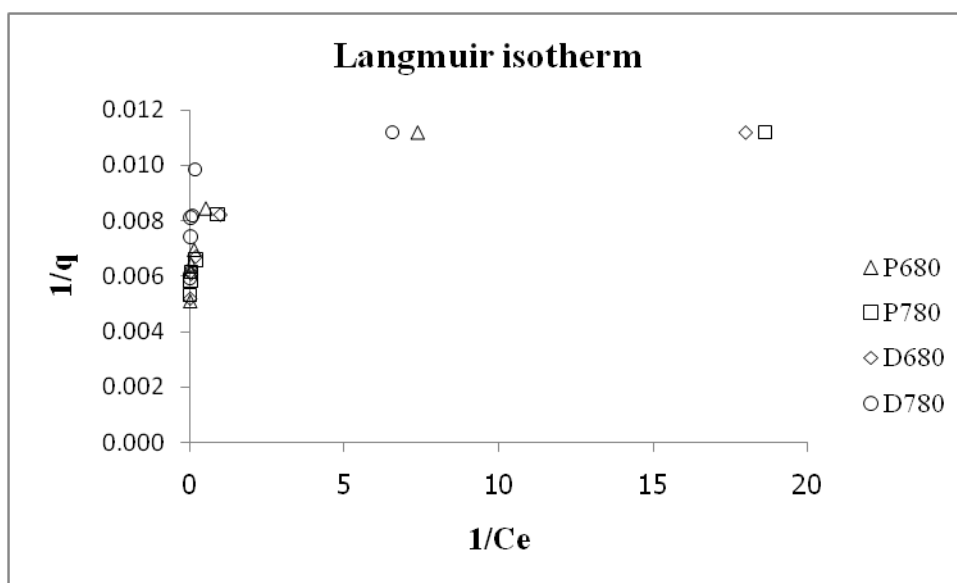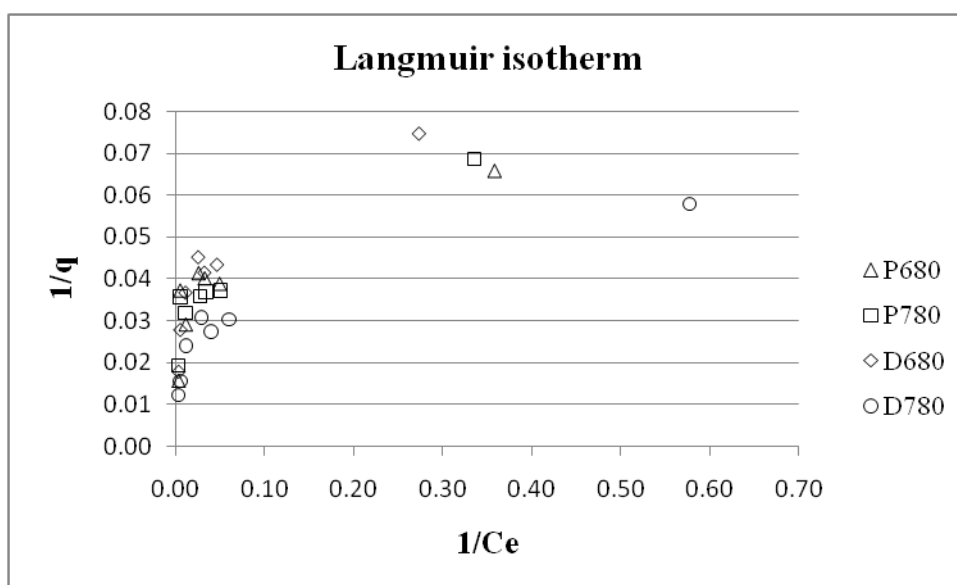

Figure 4.21 Langmuir isotherm for the adsorption of MB by synthesized zeolites (P680, P780, D680, and D780)
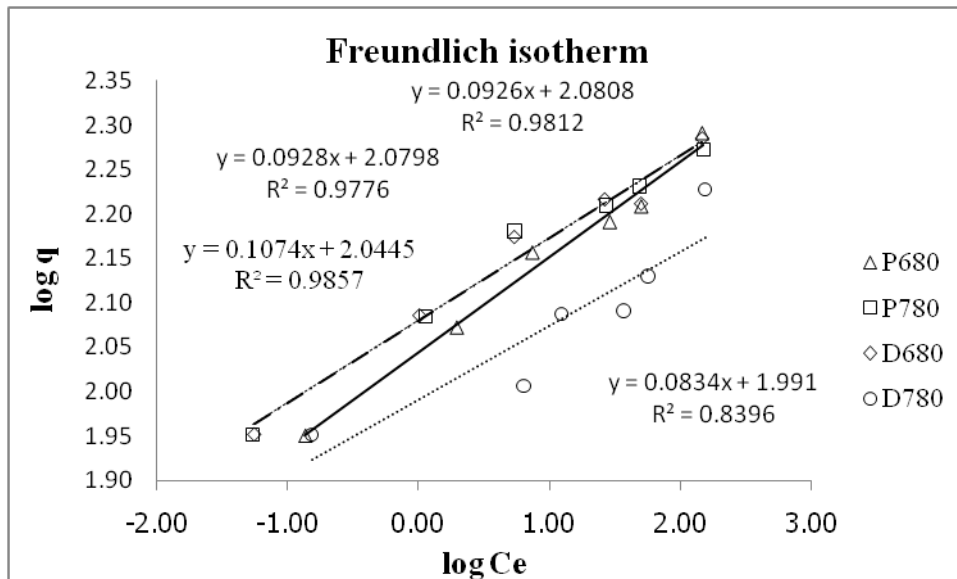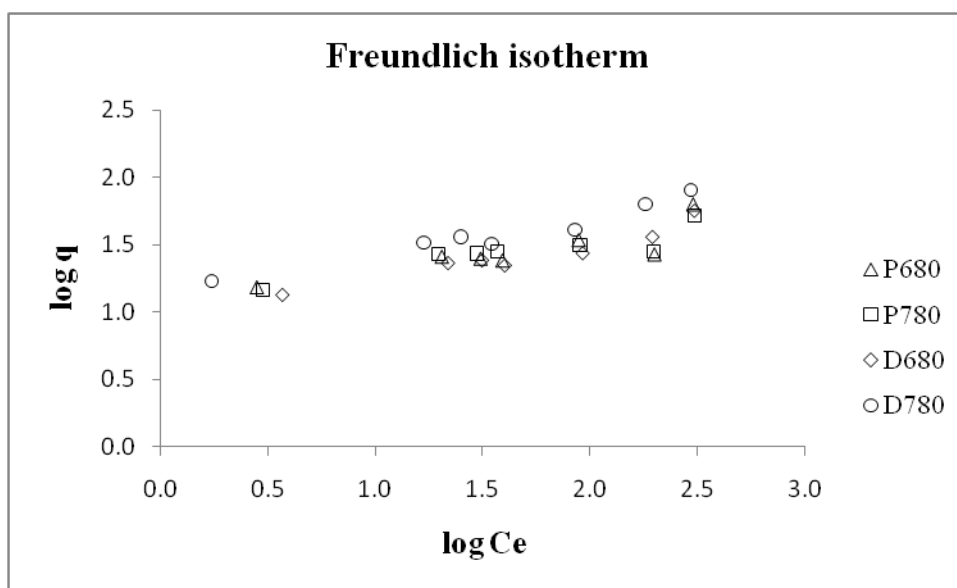
Figure 4.22 Freundlich isotherm for the adsorption of MB by synthesized zeolites (P680, P780, D680, and D780)

Table 4.9 Equations and regression coefficient (R^2) for Linear regression and Langmuir and Freundlich isotherm

Materials	Linear regression		Langmuir isotherm		Freundlich isotherm	
	equation	R^2	equation	R^2	equation	R^2
P680	y=0.1197x+19.054	0.731	y=0.0995x+0.0315	0.714	y=0.2346x+1.0612	0.717
P780	y=0.0826x+21.622	0.712	y=0.117x+0.0301	0.876	y=0.2112x+1.0992	0.793
D680	y=0.1206x+17.087	0.942	y=0.1649x+0.0317	0.805	y=0.2853x+0.945	0.907
D780	y=0.1962x+25.900	0.950	y=0.0646x+0.0217	0.832	y=0.2849x+1.1449	0.942

Table 4.10 Constant value for Linear regression and Langmuir and Freundlich isotherm

Materials	Linear regression	Langmuir isotherm		Freundlich isotherm	
	K_d	q_{max} (mg/g)	b (l/g)	K_F (mg/g)	1/n
P680	0.120	31.746	0.317	11.513	0.2346
P780	0.083	33.223	0.257	12.566	0.2112
D680	0.121	31.546	0.192	8.810	0.2853
D780	0.196	46.083	0.336	13.961	0.2849

CHAPTER V

CONCLUSIONS AND RECOMMENDATIONS

5.1 Conclusions

In this study, the optimal condition for the synthesis of zeolite from CFA and aluminum dross by alkaline fusion method was first determined. Aluminum oxide was also used for comparison with aluminum dross. Various combinations of fusion and crystallization temperature were tested. The optimal condition of zeolite synthesis from CFA and aluminum dross was at 600 °C fusion temperature and 80 °C crystallization temperature (D680). Whereas, the optimal condition for synthesizing zeolite from CFA and aluminum oxide was at 700 °C fusion temperature and 80 °C crystallization temperature (P780). These conditions were determined based on the crystalline structure and CEC of the synthesized zeolites. Zeolite A was successfully synthesized from both conditions (D680 and P780) without any detectable chemical residues. Although the CEC of aluminum dross-based zeolite was relatively lower than the one of the zeolite from aluminum oxide, both CEC values were still comparable.

The applicability of the synthesized zeolites from both optimal conditions in cadmium and MB adsorption was further investigated. Various concentrations of cadmium ranging from 25 mg/L to 200 mg/L were experimented. Up to 99.75% and 99.76% cadmium removal at 25 mg/L of cadmium were achieved by D680 and P780, respectively. Nonetheless, cadmium removal of these zeolites decreased at higher cadmium concentrations. At 200 mg/L, cadmium removal was lowered to 24.84% and 23.94% for D680 and P780, respectively. The obtained data was fitted with Freundlich isotherm, which suggests that the cadmium adsorption occurs in a heterogeneous system with reversible and multilayer adsorption.

In the case of MB adsorption, MB concentration was varied from 10 mg/L to 300 mg/L. At 10 mg/L, 64.7% and 71.26% removal was obtained by D680 and P780, respectively. With the increasing MB concentration, the MB removal of D680 and P780 was then become lower to 8.53% and 7.81 %, respectively. The soprtion capacity was increased. The collected adsorption data was analyzed with linear, Langmuir, and Freundlich isotherms. Although, the MB adsorption could not be fitted with any isotherm, the adsorption by D680 was best-fitted by Freundlich isotherms ($R^2 = 0.907$) among the three models.

Collectively, zeolites synthesized from aluminum dross exhibited comparable cadmium and MB adsoption efficiency to aluminum oxide-based zeolites. Therefore,

aluminum dross may be used as a substitution to aluminum oxide in zeolite production.

5.2 Recommendations for future study

1. Since CFA and aluminum dross can be converted to zeolite A, synthesis of other zeolites or zeotype products should also be investigated by controlling the Si/Al ratio.

2. Practically, more than one heavy metal or contaminant may occur in the same contaminated site, thus zeolite adsorption of mixed heavy metals should be studied.

3. Field or pilot scale study of environmental remediation using the synthesized zeolites should be conducted to evaluate the feasibity and practicability of these applications.

4. Cost and yield analysis of the zeolite production should be studies to determine the economic feasibility of the synthesized zeolites.

REFERENCES

lva rez-Ayuso, E., Garc a Sánchez, A., and Querol, X. 2003. Purification of metal electroplating waste waters using zeolites. Water Research 37 (20): 4855-4862.

Ronbanchob Apiratikul. 2006. Sorption of heavy metals by green macro alga, Caulerpa Lentillifera and modified zeolite from coal fly ash. Doctoral dissertation, Environmental Management, Graduate School, Chulalongkorn University.

Apiratikul, R., and Pavasant, P. 2008. Sorption of Cu2+, Cd2+, and Pb2+ using modified zeolite from coal fly ash. Chemical Engineering Journal 144 (2): 245-258.

Belviso, C., Cavalcante, F., and Fiore, S. 2010. Synthesis of zeolite from Italian coal fly ash: Differences in crystallization temperature using seawater instead of distilled water. Waste Management 30 (5): 839-847.

Berkgaut, V., and Singer, A. 1996. High capacity cation exchanger by hydrothermal zeolitization of coal fly ash. Applied Clay Science 10 (5): 369-378.

Bertin, G., and Averbeck, D. 2006. Cadmium: cellular effects, modifications of biomolecules, modulation of DNA repair and genotoxic consequences (a review). Biochimie 88 (11): 1549-1559.

Breck, D. W. 1974. Zeolite molecular sieves: Structure, Chemistry, and Use. 1974. Zeolite molecular sieves: Structure, Chemistry, and Use.

Chandrasekar, G., Kim, J., You, K.-S., Ahn, J.-W., Jun, K.-W., and Ahn, W.-S. 2009. Synthesis of hexagonal mesoporous aluminophosphate using Al dross. Korean Journal of Chemical Engineering 26 (5): 1389-1394.

Chang, H.-L., and Shih, W.-H. 2000. Synthesis of Zeolites A and X from Fly Ashes and Their Ion-Exchange Behavior with Cobalt Ions. Industrial & Engineering Chemistry Research 39 (11): 4185-4191.

Department of Agriculture. 2010. A handbook of soil analysis: chemical and physical methods. Cation exchange capacity and %Base saturation. Bangkok: Quickprint Offset. p. 46-53.

Dash, B., Das, B. R., Tripathy, B. C., Bhattacharya, I. N., and Das, S. C. 2008. Acid dissolution of alumina from waste aluminium dross. Hydrometallurgy 92 (1-2): 48-53.

David, E., and Kopac, J. 2012. Hydrolysis of aluminum dross material to achieve zero hazardous waste. Journal of Hazardous Materials 209–210 (0): 501-509.

Doğan, M., Abak, H., and Alkan, M. 2009. Adsorption of methylene blue onto hazelnut shell: Kinetics, mechanism and activation parameters. Journal of Hazardous Materials 164 (1): 172-181.

El Qada, E. N., Allen, S. J., and Walker, G. M. 2006. Adsorption of Methylene Blue onto activated carbon produced from steam activated bituminous coal: A study of equilibrium adsorption isotherm. Chemical Engineering Journal 124 (1–3): 103-110.

Engström, A., Michaëlsson, K., Vahter, M., Julin, B., Wolk, A., and Åkesson, A. 2012. Associations between dietary cadmium exposure and bone mineral density and risk of osteoporosis and fractures among women. Bone (0).

Ewais, E. M. M., Khalil, N. M., Amin, M. S., Ahmed, Y. M. Z., and Barakat, M. A. 2009. Utilization of aluminum sludge and aluminum slag (dross) for the manufacture of calcium aluminate cement. Ceramics International 35 (8): 3381-3388.

Fan, Y., Zhang, F.-S., Zhu, J., and Liu, Z. 2008. Effective utilization of waste ash from MSW and coal co-combustion power plant--Zeolite synthesis. Journal of Hazardous Materials 153 (1-2): 382-388.

Fernandes, M., Nádia, R. C., Malachini, M., and Denise, M. 2005. Synthesis of Na-A and -X zeolites from oil shale ash. Fuel 84 (18): 2289-2294.

Fernandes Machado, N. R. C., and Malachini Miotto, D. M. 2005. Synthesis of Na-A and -X zeolites from oil shale ash. Fuel 84 (18): 2289-2294.

Filipič, M. 2011. Mechanisms of cadmium induced genomic instability. Mutation Research/Fundamental and Molecular Mechanisms of Mutagenesis.

Font, O., Moreno, N., Díez, S., Querol, X., López-Soler, A., Coca, P., and García Peña, F. 2009. Differential behaviour of combustion and gasification fly ash from Puertollano Power Plants (Spain) for the synthesis of zeolites and silica extraction. Journal of Hazardous Materials 166 (1): 94-102.

Fotovat, F., Kazemian, H., and Kazemeini, M. 2009. Synthesis of Na-A and faujasitic zeolites from high silicon fly ash. Materials Research Bulletin 44 (4): 913-917.

Gross-Lorgouilloux, M., Caullet, P., Soulard, M., Patarin, J., Moleiro, E., and Saude, I. 2010. Conversion of coal fly ashes into faujasite under soft temperature

and pressure conditions. Mechanisms of crystallisation. Microporous and Mesoporous Materials 131 (1–3): 407-417.

Harvey, J. W., and Keitt, A. S. 1983. Studies of the efficacy and potential hazards of methylene blue therapy in aniline-induced methaemoglobinaemia. British Journal of Haematology 54 (1): 29-41.

Hashim, M. A., Mukhopadhyay, S., Sahu, J. N., and Sengupta, B. 2011. Remediation technologies for heavy metal contaminated groundwater. Journal of Environmental Management 92 (10): 2355-2388.

Hiraki, T., Nosaka, A., Okinaka, N., and Akiyama, T. 2009. Synthesis of Zeolite-X from Waste Metals. ISIJ International 49 (10): 1644-1648.

Hollman, G. G., Steenbruggen, G., and Janssen-Jurkovicová, M. 1999. A two-step process for the synthesis of zeolites from coal fly ash. Fuel 78 (10): 1225-1230.

Hui, K. S., and Chao, C. Y. H. 2006. Effects of step-change of synthesis temperature on synthesis of zeolite 4A from coal fly ash. Microporous and Mesoporous Materials 88 (1–3): 145-151.

Hui, K. S., Chao, C. Y. H., and Kot, S. C. 2005. Removal of mixed heavy metal ions in wastewater by zeolite 4A and residual products from recycled coal fly ash. Journal of Hazardous Materials 127 (1–3): 89-101.

Jain, C. K., and Ram, D. 1997. Adsorption of metal ions on bed sediments. Hydrological Sciences-Joumal-des Sciences Hydrologiques 42(5): 713-723.

Jamali, A. H., Mahvi, A. H., and Nazmara, S. 2009. Removal of Cadmium from Aqueous Solutions by Hazel Nut Shell. World Applied Sciences Journal 5: 16-20.

Jamil, T. S., Abdel Ghafar, H. H., Ibrahim, H. S., and Abd El-Maksoud, I. H. 2011. Removal of methylene blue by two zeolites prepared from naturally occurring Egyptian kaolin as cost effective technique. Solid State Sciences 13 (10): 1844-1851.

Järup, L., and Åkesson, A. 2009. Current status of cadmium as an environmental health problem. Toxicology and Applied Pharmacology 238 (3): 201-208.

JBMI Group Ltd. Powder Metallurgy [Online]. 2010. Available from:

http://www.jbmi.com/activities/powder-metallurgy/. [2010, November 18].

Kang, H.-Y., and Schoenung, J. M. 2005. Electronic waste recycling: A review of U.S. infrastructure and technology options. Resources, Conservation and Recycling 45 (4): 368-400.

Kang, S.-J., Egashira, K., and Yoshida, A. 1998. Transformation of a low-grade Korean natural zeolite to high cation exchanger by hydrothermal reaction with or without fusion with sodium hydroxide. Applied Clay Science 13 (2): 117-135.

Kazemian, H., Naghdali, Z., Ghaffari Kashani, T., and Farhadi, F. 2010. Conversion of high silicon fly ash to Na-P1 zeolite: Alkaline fusion followed by hydrothermal crystallization. Advanced Powder Technology 21 (3): 279-283.

Kolay, P. K., Singh, D. N., and Murti, M. V. R. 2001. Synthesis of zeolites from a lagoon ash. Fuel 80 (5): 739-745.

Majchrzak-Kuceba, I., and Nowak, W. 2005. A thermogravimetric study of the adsorption of CO2 on zeolites synthesized from fly ash. Thermochimica Acta 437 (1-2): 67-74.

Manfredi, O., Wuth, W., and Bohlinger, I. 1997. Characterizing the physical and chemical properties of aluminum dross. JOM Journal of the Minerals, Metals and Materials Society 49 (11): 48-51.

Misaelides, P. 2011. Application of natural zeolites in environmental remediation: A short review. Microporous and Mesoporous Materials 144 (1–3): 15-18.

Mokhlesi, B., Leikin, J. B., Murray, P., and Corbridge, T. C. 2003. Adult Toxicology in Critical Care*. Chest 123 (3): 897-922.

Molina, A., and Poole, C. 2004. A comparative study using two methods to produce zeolites from fly ash. Minerals Engineering 17 (2): 167-173.

Moreno, N., Querol, X., Ayora, C., Pereira, C. F., and Janssen-Jurkovicová, M. 2001. Utilization of Zeolites Synthesized from Coal Fly Ash for the Purification of Acid Mine Waters. Environmental Science & Technology 35 (17): 3526-3534.

Mulligan, C. N., Yong, R. N., and Gibbs, B. F. 2001. Remediation technologies for metal-contaminated soils and groundwater: an evaluation. Engineering Geology 60 (1–4): 193-207.

Murayama, N., Arimura, K., Okajima, N., and Shibata, J. 2009. Effect of structure-directing agent on AlPO4-n synthesis from aluminum dross. International Journal of Mineral Processing 93 (2): 110-114.

Murayama, N., Okajima, N., Yamaoka, S., Yamamoto, H., and Shibata, J. 2006. Hydrothermal synthesis of AlPO4-5 type zeolitic materials by using aluminum dross as a raw material. Journal of the European Ceramic Society 26 (4–5): 459-462.

Nascimento, M., Soares, P. S. M., and Souza, V. P. d. 2009. Adsorption of heavy metal cations using coal fly ash modified by hydrothermal method. Fuel 88 (9): 1714-1719.

Park, M., Choi, C. L., Lim, W. T., Kim, M. C., Choi, J., and Heo, N. H. 2000. Molten-salt method for the synthesis of zeolitic materials: I. Zeolite formation in alkaline molten-salt system. Microporous and Mesoporous Materials 37 (1-2): 81-89.

Penilla, R. P., Guerrero Bustos, A., and Goñi Elizalde, S. 2006. Immobilization of Cs, Cd, Pb and Cr by synthetic zeolites from Spanish low-calcium coal fly ash. Fuel 85 (5–6): 823-832.

Phanphaisan, A. 2006. Synthesis of zeolite from coal fly ash and bagasse fly ash for lead removal from industrial wastewater. M.sc. Thesis, Environmental Science, Graduate School, Chulalongkorn University.

Pollution Control Department, Ministry of Natural Resources and Environment. Pollution report of Thailand (2010) [online]. 2010. Available from: http://infofile.pcd.go.th/mgt/Report_Thai2553.pdf?CFID=8220905&CFTOKEN=39233330. [2011, June 2].

Purna Chandra Rao, G., Satyaveni, S., Ramesh, A., Seshaiah, K., Murthy, K. S. N., and Choudary, N. V. 2006. Sorption of cadmium and zinc from aqueous solutions by zeolite 4A, zeolite 13X and bentonite. Journal of Environmental Management 81 (3): 265-272.

Querol, X., Moreno, N., Umaña, J. C., Alastuey, A., Hernández, E., López-Soler, A., and Plana, F. 2002. Synthesis of zeolites from coal fly ash: an overview. International Journal of Coal Geology 50 (1-4): 413-423.

Rafatullah, M., Sulaiman, O., Hashim, R., and Ahmad, A. 2010. Adsorption of methylene blue on low-cost adsorbents: A review. Journal of Hazardous Materials 177 (1–3): 70-80.

Senthilkumaar, S., Varadarajan, P. R., Porkodi, K., and Subbhuraam, C. V. 2005. Adsorption of methylene blue onto jute fiber carbon: kinetics and equilibrium studies. Journal of Colloid and Interface Science 284 (1): 78-82.

Shawabkeh, R., Al-Harahsheh, A., Hami, M., and Khlaifat, A. 2004. Conversion of oil shale ash into zeolite for cadmium and lead removal from wastewater. Fuel 83 (7-8): 981-985.

Shigemoto, N., Hayashi, H., and Miyaura, K. 1993. Selective formation of Na-X zeolite from coal fly ash by fusion with sodium hydroxide prior to hydrothermal reaction. Journal of Materials Science 28 (17): 4781-4786.

Shih, W.-H., and Chang, H.-L. 1996. Conversion of fly ash into zeolites for ion-exchange applications. Materials Letters 28 (4–6): 263-268.

Shinzato, M. C., and Hypolito, R. 2005. Solid waste from aluminum recycling process: characterization and reuse of its economically valuable constituents. Waste Management 25 (1): 37-46.

Steenbruggen, G., and Hollman, G. G. 1998. The synthesis of zeolites from fly ash and the properties of the zeolite products. Journal of Geochemical Exploration 62 (1–3): 305-309.

Sui, Y., Wu, D., Zhang, D., Zheng, X., Hu, Z., and Kong, H. 2008. Factors affecting the sorption of trivalent chromium by zeolite synthesized from coal fly ash. Journal of Colloid and Interface Science 322 (1): 13-21.

Tanaka, H., and Fujii, A. 2009. Effect of stirring on the dissolution of coal fly ash and synthesis of pure-form Na-A and -X zeolites by two-step process. Advanced Powder Technology 20 (5): 473-479.

Tanaka, H., Matsumura, S., and Hino, R. 2004. Formation process of Na-X zeolites from coal fly ash. Journal of Materials Science 39 (5): 1677-1682.

Tu, W., Zand, B., Butalia, T. S., Ajlouni, M. A., and Wolfe, W. E. 2009. Constant rate of strain consolidation of resedimented Class F fly ash. Fuel 88 (7): 1154-1159.

U.S. Environmental Protection Agency. Guide for Industrial Waste Mannagement. [Online]. 2012. Available from: http://www.epa.gov/osw/nonhaz/industrial/guide/index.htm [2012, April 3].

Vargas, A. M. M., Cazetta, A. L., Kunita, M. H., Silva, T. L., and Almeida, V. C. 2011. Adsorption of methylene blue on activated carbon produced from flamboyant pods (Delonix regia): Study of adsorption isotherms and kinetic models. Chemical Engineering Journal 168 (2): 722-730.

Waalkes, M. P. 2003. Cadmium carcinogenesis. Mutation Research/Fundamental and Molecular Mechanisms of Mutagenesis 533 (1–2): 107-120.

Wajima, T., and Ikegami, Y. 2009. Synthesis of crystalline zeolite-13X from waste porcelain using alkali fusion. Ceramics International 35 (7): 2983-2986.

Wang, C.-F., Li, J.-S., Wang, L.-J., and Sun, X.-Y. 2008. Influence of NaOH concentrations on synthesis of pure-form zeolite A from fly ash using two-stage method. Journal of Hazardous Materials 155 (1-2): 58-64.

Wang, C., Li, J., Sun, X., Wang, L., and Sun, X. 2009. Evaluation of zeolites synthesized from fly ash as potential adsorbents for wastewater containing heavy metals. Journal of Environmental Sciences 21 (1): 127-136.

Wang, C., Li, J., Wang, L., Sun, X., and Huang, J. 2009. Adsorption of Dye from Wastewater by Zeolites Synthesized from Fly Ash: Kinetic and Equilibrium Studies. Chinese Journal of Chemical Engineering 17 (3): 513-521.

Wang, S., Soudi, M., Li, L., and Zhu, Z. H. 2006. Coal ash conversion into effective adsorbents for removal of heavy metals and dyes from wastewater. Journal of Hazardous Materials 133 (1–3): 243-251.

Wang, S., and Zhu, Z. H. 2006. Characterisation and environmental application of an Australian natural zeolite for basic dye removal from aqueous solution. Journal of Hazardous Materials 136 (3): 946-952.

Wei, M.-S., and Huang, K.-H. 2001. Recycling and reuse of industrial wastes in Taiwan. Waste Management 21 (1): 93-97.

Wimmer, G., Steinmetz, T., and Clemens, M. 2009. Reuse, Recycle, Reduce (3R) – strategies for the calculation of transient magnetic fields. Applied Numerical Mathematics 59 (3–4): 830-844.

Yaping, Y., Xiaoqiang, Z., Weilan, Q., and Mingwen, W. 2008. Synthesis of pure zeolites from supersaturated silicon and aluminum alkali extracts from fused coal fly ash. Fuel 87 (10-11): 1880-1886.

APPENDIX

Table A.1 Chemical composition of CFA and aluminum dross

Component	Coal fly ash (%wt)	Aluminum dross (%wt)
SiO_2	78.711	8.58
Al_2O_3	9.566	48.04
Na_2O	0.016	0.37
MgO	0.027	3.70
P_2O_5	2.485	0.19
SO_3	0.152	0.46
K_2O	0.793	1.62
CaO	2.136	1.65
TiO_2	0.882	0.56
Fe_2O_3	4.76	1.84
BaO	0.090	0.11
MnO_2	0.21	0.57
ZnO	0.0.3	0.78
SrO	0.075	0.00
ZrO_2	0.055	0.00
Cl	0.00	2.80
V_2O_5	0.00	< 0.01
Cr_2O_3	0.00	0.10
NiO	0.003	0.12
CuO	0.00	1.47
MnO	0.036	-
Co_3O_4	0.017	-
Rb_2O	0.004	-
CeO_2	0.055	-
WO_3	0.132	-
Y_2O_3	0.008	-

Preliminary experiment

Table A.2 Removal of cadmium by synthesized zeolite P680, P780 and D680 and D780 at 0.25, 0.5, and 1 g/L between 0 − 60 seconds (initial concentration of cadmium = 10.48 mg/L)

Sample	Zeolite/cadmium ratio	Contact time (second)	Cadmium concentration (mg/L)	% Removal
P680	0.25 g/L	5	0.158±0.11	98.49
		10	0.154±0.02	98.53
		20	0.125±0.02	98.81
		30	0.106±0.05	98.99
		60	0.077±0.03	99.27
	0.5 g/L	5	0.057±0.02	99.46
		10	0.082±0.01	99.21
		20	0.269±0.05	97.44
		30	0.034±0.01	99.68
		60	0.031±0.01	99.71
	1 g/L	5	0.056±0.03	99.47
		10	0.023±0.01	99.78
		20	0.001±0.00	100.00
		30	0.001±0.00	99.99
		60	0.003±0.00	99.98
P780	0.25 g/L	5	0.989±0.21	90.56
		10	0.600±0.22	94.27
		20	0.574±0.07	94.53
		30	0.369±0.10	96.48
		60	0.197±0.02	98.12
	0.5 g/L	5	0.417±0.05	96.02
		10	0.167±0.01	98.40
		20	0.177±0.01	98.31
		30	0.064±0.03	99.39
		60	0.040±0.02	99.62
	1 g/L	5	0.049±0.02	99.54
		10	0.020±0.02	99.81
		20	0.021±0.01	99.80
		30	0.017±0.01	99.84
		60	0.004±0.00	99.96

Sample	Zeolite/cadmium ratio	Contact time (second)	Cadmium concentration (mg/L)	% Removal
D680	0.25 g/L	5	0.761±0.26	92.74
		10	0.587±0.10	94.39
		20	0.503±0.11	95.20
		30	0.350±0.11	96.66
		60	0.322±0.07	96.93
	0.5 g/L	5	0.220±0.10	97.90
		10	0.126±0.06	98.80
		20	0.077±0.03	99.27
		30	0.046±0.04	99.56
		60	0.019±0.01	99.82
	1 g/L	5	0.071±0.06	99.33
		10	0.094±0.13	99.10
		20	0.019±0.01	99.81
		30	0.006±0.00	99.94
		60	0.009±0.01	99.91
D780	0.25 g/L	5	0.848±0.09	91.91
		10	1.033±0.04	90.14
		20	0.952±0.05	90.92
		30	0.908±0.04	91.34
		60	1.040±0.02	90.08
	0.5 g/L	5	0.159±0.02	98.48
		10	0.268±0.13	97.44
		20	0.224±0.10	97.86
		30	0.377±0.05	96.41
		60	0.575±0.06	94.52
	1 g/L	5	0.006±0.00	99.95
		10	0.034±0.01	99.68
		20	0.016±0.00	99.85
		30	0.024±0.01	99.77
		60	0.030±0.02	99.71

Effect of contact time

Table A.3 Removal of cadmium by synthesized zeolite P680, P780 and D680 and
D780 at 0.25 g/L between 0 – 540 minutes.

Sample	Contact time (min)	Cadmium concentration (mg/L)	% Removal
No sample	0	52.24	0.00
P680	5	20.71±0.12	60.36
	10	18.65±0.05	64.30
	15	16.82±0.10	67.80
	30	14.56±0.09	72.13
	60	13.79±0.10	73.60
	120	11.37±0.07	78.24
	180	8.70±0.07	83.35
	360	8.33±0.07	84.05
	540	7.03±0.08	86.54
No sample	0	51.13	0.00
P780	5	17.94±0.07	64.91
	10	15.45±0.10	69.78
	15	15.29±0.14	70.10
	30	12.79±0.09	74.99
	60	10.24±0.07	79.97
	120	8.14±0.04	84.08
	180	5.48±0.08	89.28
	360	5.05±0.05	90.13
	540	4.83±0.09	90.55
No sample	0	50.75	0.00
D680	5	15.32±0.04	69.81
	10	13.32±0.35	73.75
	15	13.79±0.16	72.83
	30	11.61±0.07	77.12
	60	7.29±0.09	85.64
	120	6.44±0.11	87.31
	180	4.62±0.12	90.90
	360	4.78±0.13	90.58
	540	4.55±0.09	91.04
No sample	0	50.44	0.00
D780	5	19.32±0.06	61.70
	10	16.85±0.08	66.59
	15	16.58±0.04	67.13
	30	14.74±0.09	70.78
	60	13.63±0.06	72.98
	120	12.44±0.15	75.34
	180	11.67±0.12	76.86
	360	11.17±0.04	77.85
	540	10.99±0.07	78.21

Effect of initial pH

Table A.4 Efficiency of synthesized zeolite at different pH

Samples	Initial pH	Cadmium concentration (mg/L)	% Removal
P680	2	50.26±0.19	1.45
	3	26.32±0.21	44.44
	4	10.85±0.32	75.90
	5	7.37±0.13	83.00
	6	3.57±0.63	89.94
	7	1.04±0.13	95.60
	8	0.16±0.09	98.72
P780	2	50.78±0.52	0.43
	3	25.02±1.94	47.19
	4	7.34±0.13	83.70
	5	5.37±0.04	87.62
	6	2.94±0.86	91.70
	7	0.62±0.23	97.41
	8	0.09±0.02	99.29
D680	2	50.22±0.59	1.54
	3	24.91±0.72	47.43
	4	8.16±0.08	81.86
	5	5.40±0.38	87.54
	6	4.65±0.07	86.88
	7	0.42±0.04	98.23
	8	0.11±0.00	99.10
D780	2	48.63±0.42	4.64
	3	32.16±0.27	32.13
	4	14.44±0.57	67.91
	5	13.32±0.08	69.30
	6	8.18±0.85	76.93
	7	1.06±0.10	95.52
	8	0.17±0.06	98.69

Effect of initial cadmium concentration

Table A.5 Removal of cadmium by synthesized zeolite P680, P780 and D680 and D780 at 25, 35, 50, 75, 100, and 200 mg/L (at initial pH 5 and contact time 3 hours)

Samples	Initial cadmium concentration (mg/L)	Sample dose (g/100 ml)	Cadmium concentration (mg/L)	% Removal	Sorption capacity (mg/g)
P680	22.62	0.0252	0.136±0.04	99.40	89.22
	31.83	0.0253	1.949±0.59	93.88	118.10
	43.38	0.0251	7.374±0.13	83.00	143.45
	67.79	0.0251	28.815±0.51	57.49	155.28
	90.91	0.0252	50.168±0.13	44.82	161.67
	196.05	0.0253	146.612±0.43	25.22	195.41
P780	22.62	0.0252	0.054±0.00	99.76	89.55
	31.83	0.0253	1.117±0.17	96.49	121.39
	43.38	0.0251	5.361±0.04	87.64	151.47
	67.79	0.0252	26.959±0.07	60.23	162.03
	90.91	0.0250	48.345±2.45	46.82	170.26
	196.05	0.0251	149.114±1.31	23.94	187.00
D680	22.62	0.0252	0.056±0.00	99.75	89.54
	31.83	0.0253	1.018±0.20	96.80	121.79
	43.38	0.0255	5.403±0.38	87.54	149.16
	67.79	0.0251	26.530±1.68	60.86	164.38
	90.91	0.0250	50.275±0.25	44.70	162.54
	196.05	0.0253	147.360±1.14	24.84	192.46
D780	22.62	0.0251	0.153±0.05	99.32	89.51
	31.83	0.0251	6.339±0.52	80.09	101.56
	43.38	0.0253	12.408±0.11	71.40	122.42
	67.79	0.0252	36.715±0.74	45.84	123.31
	90.91	0.0255	56.493±0.43	37.86	134.97
	196.05	0.0252	153.481±3.50	21.71	168.93

Adsorption isotherm of cadmium

Table A.6 Data for Linear, Langmuir, and Freundlich isotherm of cadmium

Sample	Initial Cd conc. (mg/L)	Ce (mg/L)	q (mg/g)	1/Ce	1/q	log Ce	log q
P680	22.62	0.14	89.22	7.38	0.01	-0.87	1.95
	31.83	1.95	118.10	0.51	0.01	0.29	2.07
	43.48	7.37	143.45	0.14	0.01	0.87	2.16
	67.79	28.82	155.28	0.03	0.01	1.46	2.19
	90.91	50.17	161.67	0.02	0.01	1.70	2.21
	196.05	146.61	195.41	0.01	0.01	2.17	2.29
P780	22.62	0.05	89.55	18.61	0.01	-1.27	1.95
	31.83	1.12	121.39	0.90	0.01	0.05	2.08
	43.48	5.36	151.47	0.19	0.01	0.73	2.18
	67.79	26.96	162.03	0.04	0.01	1.43	2.21
	90.91	48.34	170.26	0.02	0.01	1.68	2.23
	196.05	149.11	187.00	0.01	0.01	2.17	2.27
D680	22.62	0.06	89.54	17.99	0.01	-1.25	1.95
	31.83	1.02	121.79	0.98	0.01	0.01	2.09
	43.48	5.40	149.16	0.19	0.01	0.73	2.17
	67.79	26.53	164.38	0.04	0.01	1.42	2.22
	90.91	50.27	162.54	0.02	0.01	1.70	2.21
	196.05	147.36	192.46	0.01	0.01	2.17	2.28
D780	22.62	0.15	89.51	6.55	0.01	-0.82	1.95
	31.83	6.34	101.56	0.16	0.01	0.80	2.01
	43.48	12.41	122.42	0.08	0.01	1.09	2.09
	67.79	36.72	123.31	0.03	0.01	1.56	2.09
	90.91	56.49	134.97	0.02	0.01	1.75	2.13
	196.05	153.48	168.93	0.01	0.01	2.19	2.23

Effect of contact time

Table A.7 Removal of MB by synthesized zeolite P680, P780 and D680 and D780 at 0.25 g/L between 0 – 168 hours.

Sample	Contact time (hour)	MB concentration (mg/L)	% Removal
P680	0.25	6.271±0.10	35.95
	0.5	6.049±0.29	36.07
	1	6.012±0.17	40.77
	2	5.797±0.27	41.44
	3	5.443±0.28	42.18
	6	5.466±0.41	46.97
	9	4.472±0.22	52.18
	12	4.551±0.16	50.42
	24	3.967±0.26	58.62
	36	3.236±0.14	65.74
	48	2.600±0.31	74.62
	60	2.814±0.66	72.11
	72	1.527±0.12	78.91
	96	1.855±0.16	81.32
	120	1.787±0.07	79.18
	144	1.806±0.13	80.88
	168	1.815±0.17	77.55
P780	0.25	4.098±0.26	58.15
	0.5	3.745±0.21	60.42
	1	3.662±0.42	63.93
	2	3.220±0.31	67.48
	3	2.873±0.19	69.49
	6	2.922±0.39	71.65
	9	2.669±0.16	71.46
	12	2.477±0.26	73.01
	24	2.217±0.26	76.87
	36	1.950±0.20	79.35
	48	2.069±0.25	79.80
	60	2.065±0.37	79.53
	72	1.417±0.28	80.43
	96	1.954±0.39	80.33
	120	1.657±0.21	80.70
	144	1.842±0.34	80.50
	168	1.570±0.31	80.57

Sample	Contact time (hour)	MB concentration (mg/L)	% Removal
D680	0.25	6.516±0.42	33.44
	0.5	6.330±0.32	33.10
	1	6.657±0.37	34.42
	2	5.995±0.47	39.45
	3	5.371±0.33	42.95
	6	5.394±0.20	47.66
	9	5.052±0.03	45.98
	12	4.120±0.31	55.12
	24	4.041±0.26	57.84
	36	3.491±0.40	63.04
	48	3.588±0.38	64.98
	60	3.435±0.33	65.95
	72	2.376±0.21	67.17
	96	2.973±0.24	70.07
	120	2.560±0.22	70.18
	144	2.815±0.23	70.20
	168	2.434±0.17	69.89
D780	0.25	6.322±0.03	35.43
	0.5	5.468±0.06	42.21
	1	5.690±0.32	43.95
	2	4.782±0.35	51.70
	3	4.522±0.26	51.97
	6	4.395±0.23	57.36
	9	3.735±0.28	60.06
	12	3.182±0.17	65.34
	24	2.946±0.30	69.27
	36	2.458±0.05	73.98
	48	2.265±0.03	77.89
	60	2.235±0.17	77.85
	72	2.376±0.96	82.20
	96	1.725±0.09	82.63
	120	1.355±0.20	84.21
	144	1.449±0.16	84.66
	168	1.260±0.11	84.42

Effect of initial MB concentration

Table A.8 Removal of MB by synthesized zeolite P680, P780 and D680 and D780 at 10, 30, 40, 50, 100, 200, and 300 mg/L (contact time 5 days)

Samples	Initial MB concentration (mg/L)	Sample dose (g/50 ml)	MB concentration (mg/L)	% Removal	Sorption capacity (mg/g)
P680	10.39	0.0250	2.797±0.07	73.08	15.19
	33.29	0.0252	20.321±0.49	38.95	25.73
	43.42	0.0254	30.772±0.52	29.13	24.90
	51.01	0.0251	38.890±0.76	23.76	24.14
	105.41	0.0252	88.123±1.38	16.40	34.30
	211.80	0.0251	198.324±3.00	6.36	26.84
	332.62	0.0252	300.528±6.86	9.65	63.67
P780	10.39	00254	2.986±0.20	71.26	14.57
	33.29	0.0253	19.697±0.37	40.83	26.86
	43.42	0.0254	29.646±0.70	31.73	27.12
	51.01	0.0252	36.932±0.52	27.60	27.93
	105.41	0.0252	89.541±0.51	15.06	31.49
	211.80	0.0252	197.657±0.23	6.68	28.06
	332.62	0.0251	306.628±2.43	7.81	51.77
D680	10.39	0.0251	3.668±0.22	64.70	13.39
	33.29	0.0252	21.662±0.53	34.92	23.07
	43.42	0.0254	31.167±1.71	28.23	24.13
	51.01	0.253	39.803±0.18	21.97	22.15
	105.41	0.0250	91.770±0.77	12.94	27.28
	211.80	0.0250	193.788±1.39	8.50	36.02
	332.62	0.0252	304.241±3.22	8.53	56.30
D780	10.39	0.0251	1.733±0.02	83.32	17.25
	33.29	0.0251	16.738±1.37	49.72	32.97
	43.42	0.0253	24.991±0.81	42.45	36.43
	51.01	0.0252	34.649±0.69	32.08	32.46
	105.41	0.0253	84.409±1.24	19.93	41.51
	211.80	0.0251	179.645±4.09	15.18	64.05
	332.62	0.0252	291.776±6.95	12.28	81.03

Adsorption isotherm of MB

Table A.9 Data for Linear, Langmuir, and Freundlich isotherm of MB

Sample	Initial MB conc. (mg/L)	Ce (mg/L)	q (mg/g)	1/Ce	1/q	log Ce	log q
P680	10.39	2.80	15.19	0.36	0.07	0.45	1.18
	33.29	20.32	25.73	0.05	0.04	1.31	1.41
	43.42	30.77	24.90	0.03	0.04	1.49	1.40
	51.01	38.89	24.14	0.03	0.04	1.59	1.38
	105.41	88.12	34.30	0.01	0.03	1.95	1.54
	211.80	198.32	26.84	0.01	0.04	2.30	1.43
	332.62	300.53	63.67	0.00	0.02	2.48	1.80
P780	10.39	2.99	14.57	0.33	0.07	0.48	1.16
	33.29	19.70	26.86	0.05	0.04	1.29	1.43
	43.42	29.65	27.12	0.03	0.04	1.47	1.43
	51.01	36.93	27.93	0.03	0.04	1.57	1.45
	105.41	89.54	31.49	0.01	0.03	1.95	1.50
	211.80	197.66	28.06	0.01	0.04	2.30	1.45
	332.62	306.63	51.77	0.00	0.02	2.49	1.71
D680	10.39	3.67	13.39	0.27	0.07	0.56	1.13
	33.29	21.66	23.07	0.05	0.04	1.34	1.36
	43.42	31.17	24.13	0.03	0.04	1.49	1.38
	51.01	39.80	22.15	0.03	0.05	1.60	1.35
	105.41	91.77	27.28	0.01	0.04	1.96	1.44
	211.80	193.79	36.02	0.01	0.03	2.29	1.56
	332.62	304.24	56.30	0.00	0.02	2.48	1.75
D780	10.39	1.73	17.25	0.58	0.06	0.24	1.24
	33.29	16.74	32.97	0.06	0.03	1.22	1.52
	43.42	24.99	36.43	0.04	0.03	1.40	1.56
	51.01	34.65	32.46	0.03	0.03	1.54	1.51
	105.41	84.41	41.51	0.01	0.02	1.93	1.62
	211.80	179.64	64.05	0.01	0.02	2.25	1.81
	332.62	291.78	81.03	0.00	0.01	2.47	1.91

(a)

File: RM.raw - Type: 2Th/Th locked - Start: 5.000 ° - End: 80.000 ° - Step: 0.050 ° - Step time: 3. s - Temp.: 25 °C (Room) -
78-1254 (C) - Quartz lpha, syn - SiO2 - Y: 94.94 % - d x by: 1. - WL: 1.5406 - Hexagonal - a 4.88170 - b 4.88170 - c 5.3753
06-0259 (D) - Mullite - 3Al2O3·2SiO2 - Y: 16.67 % - d x by: 1. - WL: 1.5406 - Orthorhombic - a 14.88000 - b 15.18000 - c 5.

(b)

File: sample 24.raw - Type: 2Th/Th locked - Start: 5.000 ° - End: 80.000 ° - Step: 0.020 ° - Step ti   00-048-1581 (I) - Aluminum Oxide Nitride - Al8O3N6 - Hexagonal
00-004-0787 (*) - Aluminum, syn [NR] - Al - Cubic
00-027-1402 (*) - Silicon, syn - Si - Cubic
00-010-0173 (I) - Corundum, syn - Al2O3 - Hexagonal (Rh)
00-025-1133 (*) - Aluminum Nitride - AlN - Hexagonal
00-031-0701 (I) - Lithium Aluminum Chromium Oxide - LiAl4.4Cr0.6O8 - Cubic
00-039-1076 (I) - Cadmium Aluminum Silicide - Cd1.00Al1.04Si1.92 - Orthorhombic
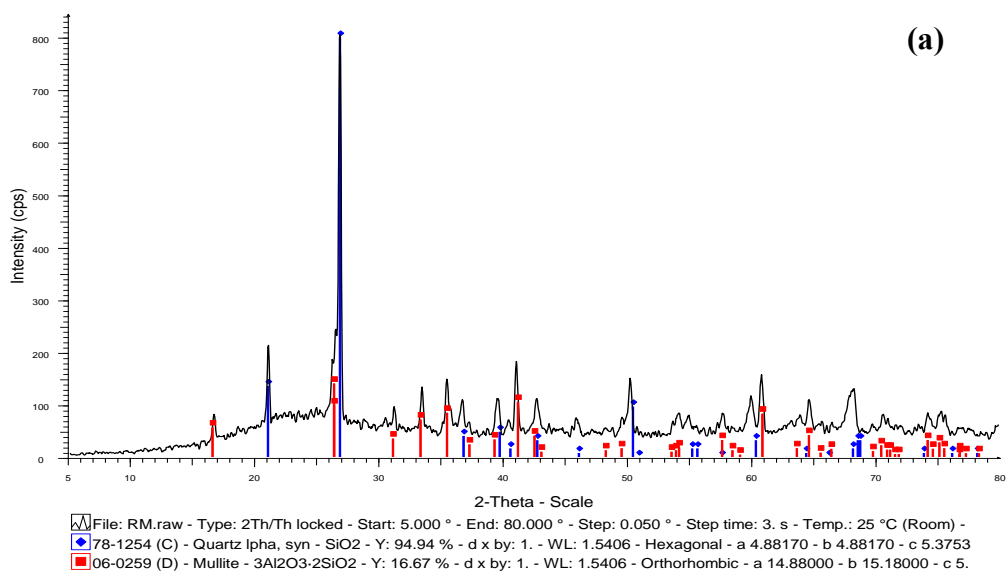
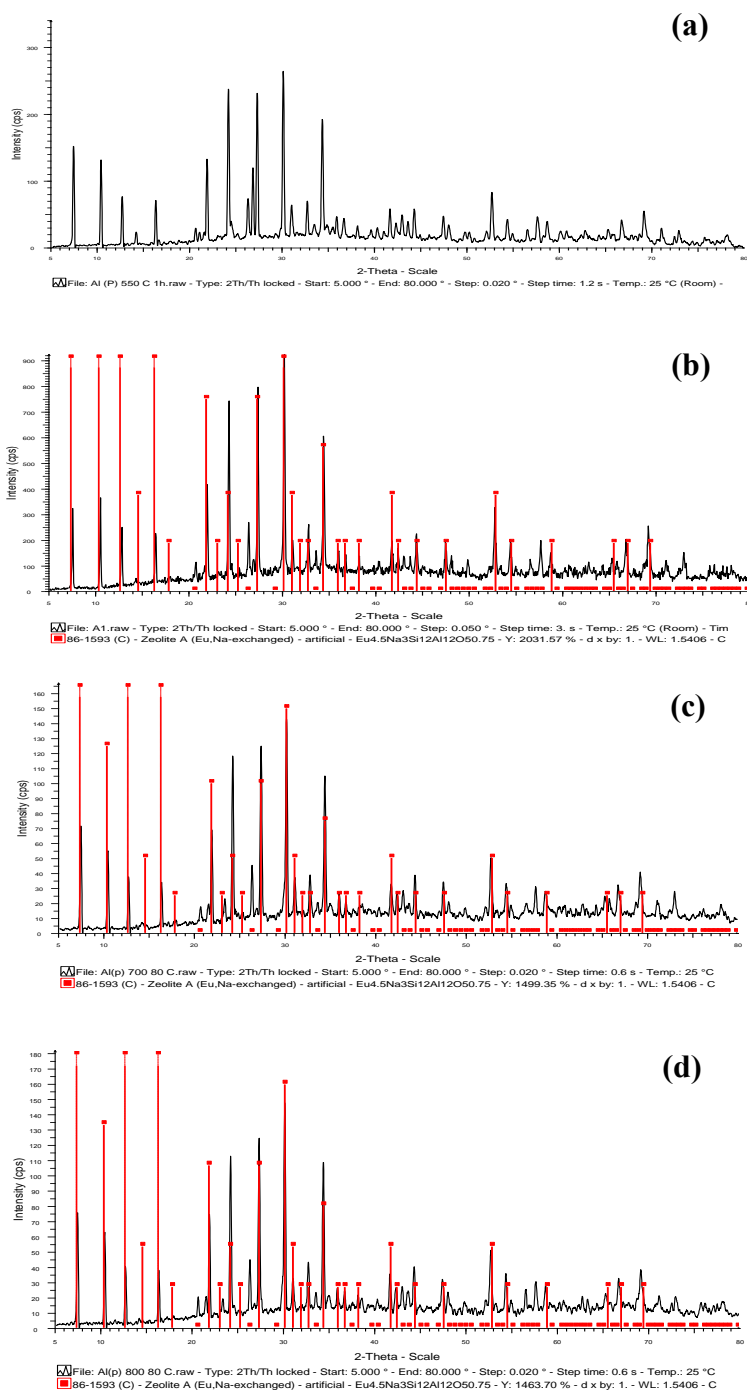**Figure A.1** XRD patterns of raw materials (a) CFA and (b) aluminum dross

Figure A.2 XRD patterns of synthesized zeolite using aluminum oxide at different fusion temperature and 80 ˚C crystallization temperature (a) 550 ˚C, (b) 600 ˚C, (c) 700 ˚C, and (d) 800 ˚C
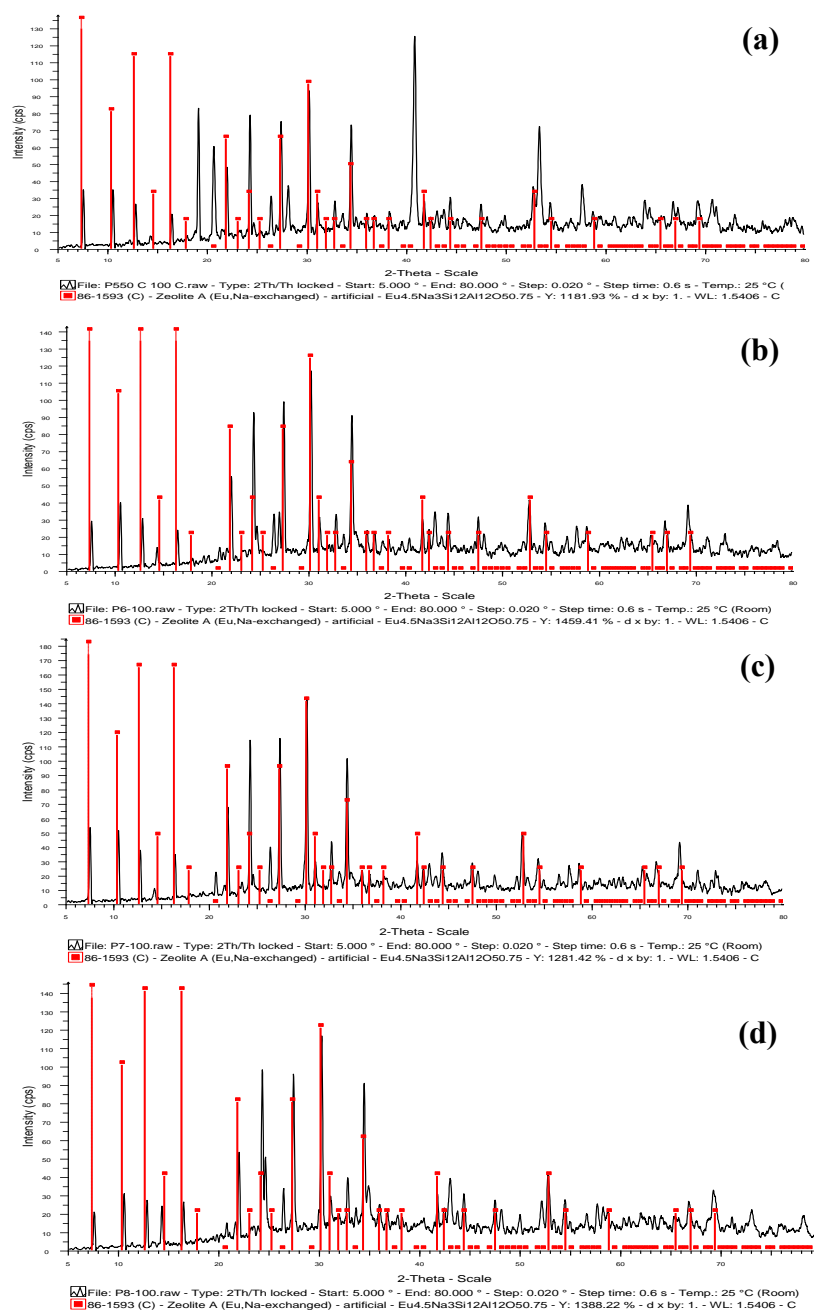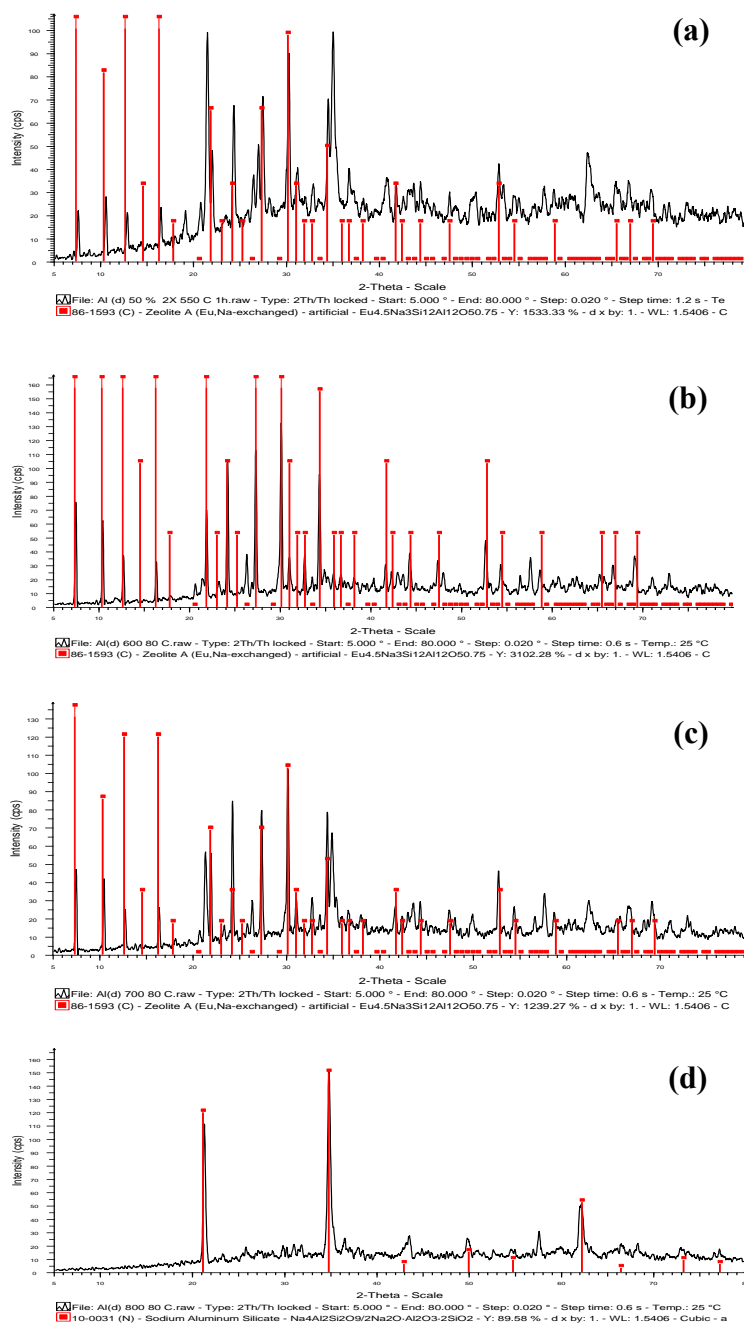
Figure A.3 XRD patterns of synthesized zeolite using aluminum oxide at different fusion temperature and 100 ˚C crystallization temperature (a) 550 ˚C, (b) 600 ˚C, (c) 700 ˚C, and (d) 800 ˚C

Figure A.4 XRD patterns of synthesized zeolite using aluminum dross at different fusion temperature and 80 ˚C crystallization temperature (a) 550 ˚C, (b) 600 ˚C, (c) 700 ˚C, and (d) 800 ˚C
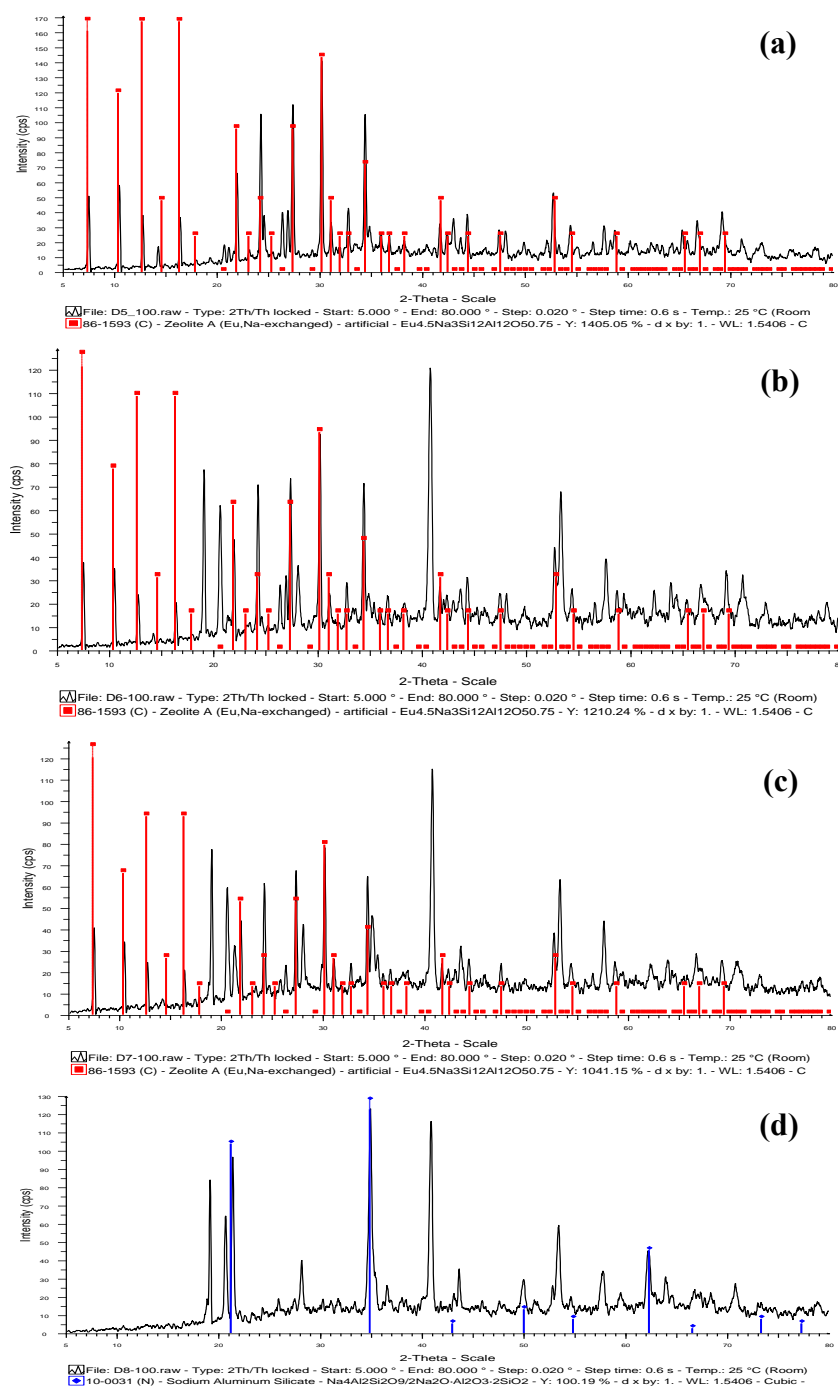
Figure A.5 XRD patterns of synthesized zeolite using aluminum dross at different fusion temperature and 100 ˚C crystallization temperature (a) 550 ˚C, (b) 600 ˚C, (c) 700 ˚C, and (d) 800 ˚C

Calculation of silica to aluminum to NaOH ratio for zeolite synthesis

Silica was obtained from CFA, whereas aluminum was obtained from CFA, and either chemical aluminum (Al_2O_3) or aluminum dross. Prior to use, the aluminum dross was thoroughly homogenized. During the calculation of the molar ratio, it was assumed that aluminum was resulted solely from the aluminum oxide content of the aluminum dross.

1. Silica : chemical aluminum (Al_2O_3) : NaOH = 1:1:1.2

    For 20 g of CFA;

$$Si\ content\ =\ \frac{78.71x20}{100}\ =\ 15.74\ g$$

$$Al\ content\ =\ \frac{9.57x20}{100}\ =\ 1.914\ g$$

Thus the required amount of Al_2O_3 = 15.74 – 1.914

= 13.83 g

2. Silica : aluminum dross : NaOH = 1:1:1.2

    For 20 g of CFA;

$$Si\ content\ =\ \frac{78.71x20}{100}\ =\ 15.74\ g$$

$$Al\ content\ =\ \frac{9.57x20}{100}\ =\ 1.914\ g$$

Thus the required amount of aluminum dross = $(15.74 – 1.914) \times \frac{100}{48.04}$

= 28.78 g

BIOGRAPHY

Miss Napasawan Khawnuan was born on July 18th, 1987 in Bangkok, Thailand. She graduated with Bachelor's Degree in Environmental Science from Faculty of Science, Silpakorn University in 2008. She pursued her Master's Degree in Environmental Management (International Program) at Chulalongkorn University. She presented a part of her research at the 2011 International Winter Conference on Environmental Innovations and Sustainability on January 29th, 2011 in Beppu, Oita, Japan under the topic of "Synthesis of zeolite from coal fly ash (CFA) with aluminum dross using alkali fusion".